© 2016. Published by The Company of Biologists Ltd | Development (2016) 143, 1710-1720 doi:10.1242/dev.127647

STEM CELLS AND REGENERATION

RESEARCH ARTICLE

The ADP-ribose polymerase Tankyrase regulates adult intestinal stem cell proliferation during homeostasis in *Drosophila*

Zhenghan Wang[1], Ai Tian[1], Hassina Benchabane[1], Ofelia Tacchelly-Benites[1], Eungi Yang[1], Hisashi Nojima[2] and Yashi Ahmed[1,*]

ABSTRACT

Wnt/β-catenin signaling controls intestinal stem cell (ISC) proliferation, and is aberrantly activated in colorectal cancer. Inhibitors of the ADP-ribose polymerase Tankyrase (Tnks) have become lead therapeutic candidates for Wnt-driven cancers, following the recent discovery that Tnks targets Axin, a negative regulator of Wnt signaling, for proteolysis. Initial reports indicated that Tnks is important for Wnt pathway activation in cultured human cell lines. However, the requirement for Tnks in physiological settings has been less clear, as subsequent studies in mice, fish and flies suggested that Tnks was either entirely dispensable for Wnt-dependent processes *in vivo*, or alternatively, had tissue-specific roles. Here, using null alleles, we demonstrate that the regulation of Axin by the highly conserved *Drosophila* Tnks homolog is essential for the control of ISC proliferation. Furthermore, in the adult intestine, where activity of the Wingless pathway is graded and peaks at each compartmental boundary, Tnks is dispensable for signaling in regions where pathway activity is high, but essential where pathway activity is relatively low. Finally, as observed previously for Wingless pathway components, Tnks activity in absorptive enterocytes controls the proliferation of neighboring ISCs non-autonomously by regulating JAK/STAT signaling. These findings reveal the requirement for Tnks in the control of ISC proliferation and suggest an essential role in the amplification of Wnt signaling, with relevance for development, homeostasis and cancer.

KEY WORDS: Axin, Signal Transduction, Tankyrase, Wingless, Wnt, β-catenin

INTRODUCTION

The Wnt/β-catenin signal transduction pathway regulates intestinal stem cell (ISC) self-renewal in mammals, whereas conditional inactivation of Wnt signaling results in the loss of intestinal proliferative crypts and associated ISCs (Fevr et al., 2007; Ireland et al., 2004; Korinek et al., 1998; van Es et al., 2012). Conversely, the aberrant activation of Wnt signaling triggers development of the vast majority of colorectal carcinomas (Korinek et al., 1997; Morin et al., 1997). Despite our relatively detailed understanding of essential steps in Wnt pathway activation (Clevers and Nusse, 2012; MacDonald et al., 2009), the identification of clinically effective small-molecule inhibitors to treat Wnt-driven cancers has been challenging (Lum and Clevers, 2012). Therefore, the discovery that the ADP-ribose polymerase Tankyrase (Tnks) targets Axin, a negative regulator of Wnt signaling, for proteolysis was a breakthrough (Huang et al., 2009). Small-molecule Tnks inhibitors that disrupted Wnt signaling in cultured human cells (Chen et al., 2009; Huang et al., 2009; Lau et al., 2013; Waaler et al., 2012) and reduced the growth of colonic adenomas in mouse models (Lau et al., 2013; Waaler et al., 2012) have been identified, suggesting a promising new strategy for the treatment of Wnt-driven cancers.

However, the requirement for Tnks in physiological settings has remained less clear, because *in vivo* studies suggested either that Tnks was dispensable for Wnt-dependent processes, or conversely, that Tnks had tissue- or stage-specific roles. For example, in flies, genetic inactivation of Tnks resulted in no Wingless-dependent developmental phenotypes unless Axin was simultaneously overexpressed at levels high enough to abrogate Wingless signaling (Feng et al., 2014). Similarly, no defects in Wnt-dependent processes were observed after treatment of fish with Tnks inhibitors during embryonic development (Huang et al., 2009), but these inhibitors disrupted the regeneration of adult fins following injury (Chen et al., 2009; Huang et al., 2009), a process that is dependent on Wnt and several other signaling pathways (Wehner and Weidinger, 2015). Finally, functional redundancy exists between the two Tnks homologs in mice (Chiang et al., 2008) and double mutants displayed embryonic lethality, but no overt Wnt-related phenotypes (see also Discussion in Qian et al., 2011). However, a mutation in mouse *Axin2* that is predicted to disrupt Tnks-dependent ADP-ribosylation paradoxically resulted in both hyperactivating and inhibiting effects on Wnt signaling in the primitive streak that were dependent on developmental stage. These opposing effects were also observed following treatment with Tnks inhibitors, suggesting complex roles in embryonic development (Qian et al., 2011). The mechanistic basis for these disparate effects of Tnks inhibition in the different *in vivo* models remains unknown.

In this study, we have focused on the function of Tnks in the adult *Drosophila* midgut, which, because of its simplicity and similarity to the vertebrate intestine, has emerged as a powerful model for studying intestinal homeostasis, regeneration and tumorigenesis (Jiang and Edgar, 2011). The activation of the Wingless pathway is graded along the length of the adult intestine, peaking at each of the boundaries between compartments and present at lower levels within compartments (Buchon et al., 2013; Tian et al., 2016). During homeostasis, Wingless signaling regulates ISC proliferation (Buchon et al., 2013; Tian et al., 2016). Here, we demonstrate that the regulation of Axin by Tnks is required for the control of adult ISC proliferation. Importantly, we find that Tnks is essential for Wingless target gene activation within regions of the gut where the Wingless pathway is activated at relatively low levels, but dispensable where Wingless pathway activity is high. Our findings suggest that, like Wingless pathway components, the role of Tnks is crucial for the non-autonomous control of Janus kinase/

[1]Department of Genetics and the Norris Cotton Cancer Center, Geisel School of Medicine at Dartmouth College, Hanover, NH 03755, USA. [2]The Francis Crick Institute, Mill Hill Laboratory, London NW7 1AA, UK.

*Author for correspondence (yfa@dartmouth.edu)

Received 22 June 2015; Accepted 8 March 2016

Development (2016) 143, 1710-1720 doi:10.1242/dev.127647

signal transducer and activator of transcription (JAK/STAT) signaling in ISCs, and thereby essential to maintain intestinal homeostasis. Our findings provide the first *in vivo* evidence using null alleles that regulation of Axin by Tnks is essential for Wingless target gene activation under physiological conditions. The requirement for Tnks is spatially restricted within the graded range of Wnt pathway activation, suggesting that the context-dependent requirements for Tnks reflect an essential role in the amplification of signaling following Wnt stimulation.

RESULTS

Tnks is essential for control of ISC proliferation in the adult midgut

Fly genomes encode only one Tnks, which is highly conserved; the overall similarity between the *Drosophila melanogaster* and human TNKS1 and TNKS2 proteins is 79% (Fig. 1A). Like the human TNKS proteins, the single *Drosophila* Tnks contains five Ankyrin repeat clusters (ARC), a sterile α motif (SAM) and a poly(ADP-ribose) polymerase (PARP) domain (Fig. 1A) (Sbodio et al., 2002; Smith et al., 1998). ARC2, ARC4 and ARC5 in the mammalian TNKS proteins, which bind axin directly (Morrone et al., 2012), share between 91% and 93% similarity with the corresponding fly Tnks ARCs, suggesting evolutionary conservation in function.

To examine Tnks function *in vivo*, we isolated *Drosophila Tnks* mutants using either imprecise excision or hybrid element insertion (Pare et al., 2009; Parks et al., 2004) of transposons flanking the *Tnks* gene. We identified two alleles: $Tnks^{503}$, a deletion that eliminates the *Tnks* transcription and translation initiation sites and $Tnks^{19}$, a deletion that eliminates the *Tnks* gene entirely (Fig. 1B). Both alleles are null, as revealed by immunoblots of larval lysates using a Tnks antibody (Fig. 1C). Although TNKS function is essential for viability in mice, *Tnks* null mutant flies were viable, eclosed at a normal rate and displayed no external morphological defects under standard lab conditions, consistent with previous findings (Feng et al., 2014). However, by comparison with controls, *Tnks* mutant adults displayed markedly increased mortality when fed only water supplemented with sucrose (Fig. 1D).

We postulated that the high mortality in *Tnks* mutants might arise from digestive tract defects that compromised their ability to absorb nutrients and thus examined their guts to address this possibility. In the *Drosophila* midgut, the ISCs give rise to two types of daughter progenitors, the undifferentiated enteroblast (EB) and the pre-enteroendocrine (pre-EE) cell (Beehler-Evans and Micchelli, 2015; Biteau and Jasper, 2014; Micchelli and Perrimon, 2006; Ohlstein and Spradling, 2006; Zeng and Hou, 2015; Zielke et al., 2014). EBs and pre-EEs differentiate into absorptive enterocytes (ECs) and secretory enteroendocrine (EE) cells, respectively. We identified midgut progenitor cells by their expression of the transcription factor *escargot* (*esg*) (Micchelli and Perrimon, 2006). In controls, progenitor cells were distributed evenly along the length of the midgut, as revealed by the *esg-Gal4, UAS-GFP* (*esg>GFP*) reporter (Fig. 2A-C). By contrast, *Tnks* null mutants displayed a markedly increased number of progenitor cells compared with controls, an effect that was most pronounced in the posterior midgut (Fig. 2D-F). Furthermore, multi-cell clusters of progenitor cells were detected frequently in *Tnks* mutants, but not in controls (Fig. 2D-F, arrows).

To distinguish ISCs from the other progenitor cell types, we stained wild-type or *Tnks* mutant midguts with the ISC-specific marker Delta (Dl) (Ohlstein and Spradling, 2007). We observed a marked increase in the number of ISCs in the midguts of *Tnks* mutants compared with wild-type flies (Fig. 2G-M). Notably, the increase in the number of progenitor cells in *Tnks* mutants became more severe with age. For example, by 14 days after eclosion, there was a large increase in the number of $esg>GFP^{+}$ cells in the midgut of *Tnks* mutants compared with controls (Fig. S1A,C). Immunostaining with phospho-histone H3 (pH3) antibody revealed a significant increase in $pH3^{+}$ cells in *Tnks* mutant midguts, indicating increased numbers of cells undergoing mitosis (Fig. 2N and Fig. S1B,D). Together, these findings indicate that loss of Tnks results in an aberrantly increased rate of ISC proliferation, and consequently, an increased number of progenitor cells in the adult midgut.

To determine whether Tnks is essential for regulating ISC proliferation during adulthood, we used the MARCM (mosaic analysis with a repressible cell marker) technique (Lee and Luo,

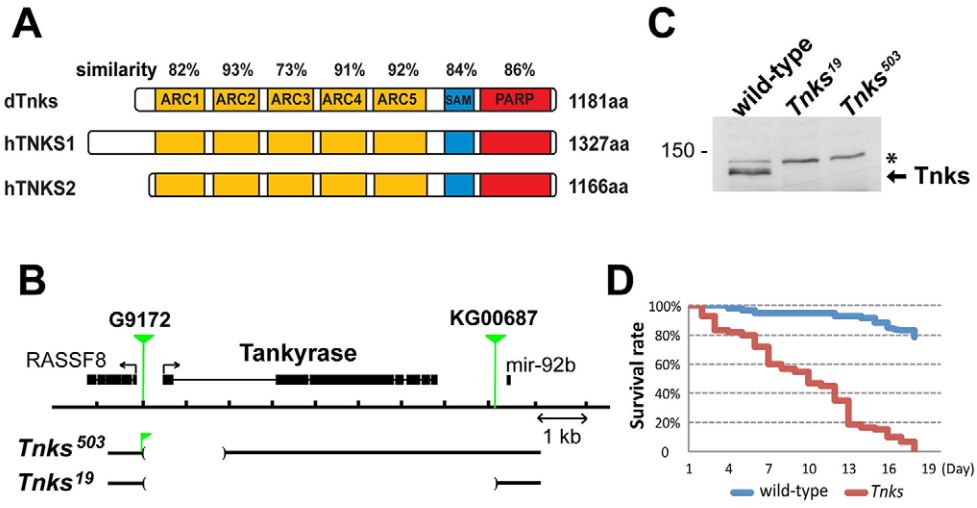

Fig. 1. *Tnks* mutants display increased mortality under reduced nutrient conditions. (A) Schematic representation of domains in *Drosophila* Tnks and human TNKS1 and TNKS2. ARC, Ankyrin repeat cluster; SAM, sterile alpha motif; PARP, poly-ADP-ribose polymerase catalytic domain. Percentage similarity between dTnks and hTNKS is indicated above each domain. (B) Schematic representation of the *Tnks* genomic region and deletions in two *Drosophila Tnks* null mutants, $Tnks^{19}$ and $Tnks^{503}$. A fragment of the P element *G9172* remains in the $Tnks^{503}$ mutant. (C) *Tnks* null mutants confirmed by immunoblotting. Immunoblots using an antibody against Tnks detect endogenous Tnks in wild-type flies, but not in *Tnks* null mutants. A nonspecific band serves as a control for loading (asterisk). (D) $Tnks^{19/503}$ mutant flies show increased mortality compared with wild-type flies when fed with 5% sucrose solution. *n*=60 for each genotype.

Development (2016) 143, 1710-1720 doi:10.1242/dev.127647

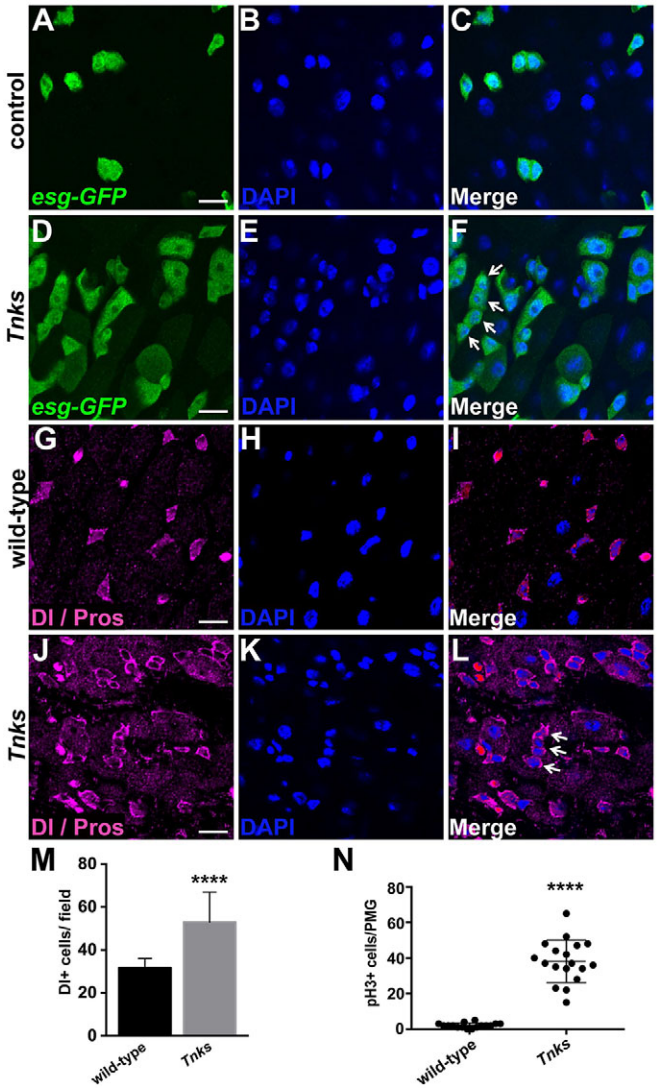

Fig. 2. Tnks prevents overproliferation of ISCs. (A-F) *Tnks* mutant flies have an increased number of progenitor cells that form clusters (arrow). Midguts of 5-day-old female expressing *esg-Gal4, UAS-GFP (esg>GFP)* stained with anti-GFP (green) and DAPI. In control ($Tnks^{503/+}$) midguts (A-C), $esg{>}GFP^{+}$ progenitor cells are evenly spaced. (G-L) *Tnks* mutant flies have an increased number of ISCs that form clusters (arrow). Midguts of 5-day-old wild-type or $Tnks^{19/503}$ null mutant flies stained with anti-Delta and anti-Prospero antibodies to mark ISCs and EEs, respectively. Scale bars: 10 µm. (M) Quantification of the relative number of $Delta^{+}$ cells in 5-day-old wild-type (n=17) or $Tnks^{19/503}$ mutant flies (n=19). (N) Quantification of $pH3^{+}$ cells in posterior midgut (PMG) of 14-day-old wild-type (n=16) or $Tnks^{19/503}$ mutant flies (n=18). Values are presented as means±s.d. ****P<0.0001 (t-test).

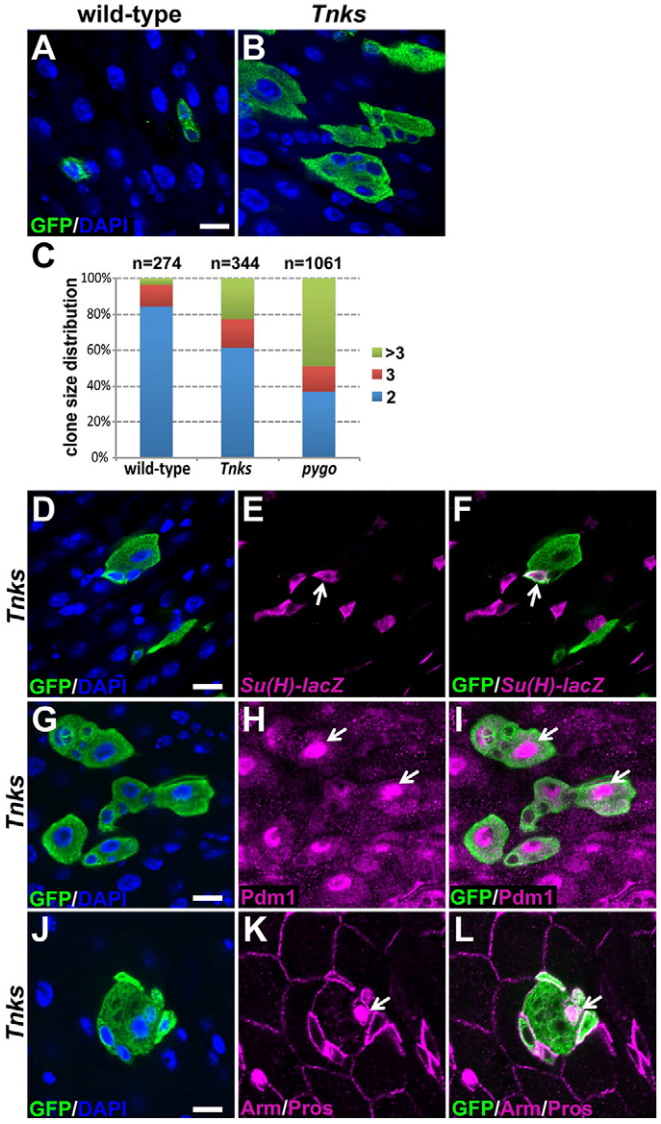

Fig. 3. Tnks regulates ISC proliferation but not differentiation during homeostasis. MARCM clones (marked by GFP) of indicated genotypes, stained with anti-GFP (green) and DAPI. $Tnks^{19}$ flies (B) have increased number of multi-cell clones compared with wild-type flies (A). (C) Quantification of clone size for wild-type, $Tnks^{19}$ or $pygo^{S123}$ ISC lineages in posterior midguts. Number of clones examined is indicated. (D-F) *Tnks* mutant ISCs can give rise to transient undifferentiated EBs (arrow). $Tnks^{19}$ clones are marked by GFP (green) and EBs by *Su(H)-lacZ* (magenta). (G-I) *Tnks* mutant ISCs can differentiate into ECs (arrow). (J-L) *Tnks* mutant ISCs can differentiate into EE cells (arrow). Clones were induced in adults on the day of eclosion and analyzed 4 days later. Scale bars: 10 µm.

2001) to induce marked clones of either wild-type or *Tnks* mutant cells. We excluded transient clones by restricting our analysis to clones in the posterior midgut that contained two or more cells. When wild-type clones were induced on the day of eclosion and analyzed 4 days later, only 3.6% of the clones contained more than three cells (Fig. 3A,C). By contrast, the proportion of multi-cell clones (n>3) increased significantly following Tnks inactivation, to 22.7% (Fig. 3B,C). To address the possibility that the increased number of ISCs in *Tnks* mutants resulted from a block in their differentiation, we stained *Tnks* mutant clones for the presence of EBs, ECs and EE cells with the cell type-specific markers Suppressor of Hairless (*Su(H)-lacZ*), Pdm1 and Prospero, respectively (Lee et al., 2009; Micchelli and Perrimon, 2006; Ohlstein and Spradling, 2006). We found that EBs, ECs and EE cells were all present within *Tnks* mutant clones, indicating that Tnks is not essential for epithelial cell differentiation in the midgut (Fig. 3D-L). Therefore, Tnks is dispensable for cell differentiation, but essential for the control of ISC proliferation during homeostatic conditions in the adult gut.

A spatially restricted requirement for Tnks within the graded activation of the Wingless pathway promotes signaling in the adult midgut

Wingless signaling was initially proposed to maintain the ISC population by preventing differentiation (Lin et al., 2008). However,

Development (2016) 143, 1710-1720 doi:10.1242/dev.127647

more recent studies have revealed that the activation of Wingless signaling in ISCs had only mild effects on tissue self-renewal under basal homeostatic conditions, but had a major role in the response of ISCs to injury (Cordero et al., 2012; Lee et al., 2009). Recently, we reported the role of Wingless signaling in intestinal homeostasis during early adulthood (Tian et al., 2016). Our findings, based on null alleles and RNAi-mediated knockdown of multiple Wingless pathway core components, revealed that the activation of the Wingless pathway in ECs non-autonomously inhibits ISC proliferation under basal conditions during intestinal homeostasis.

Therefore, we hypothesized that defects in the regulation of ISC proliferation observed in *Tnks* mutants could have resulted from inhibition of Wingless signaling. To test this hypothesis, we compared the effects of inactivation of either the essential Wingless signaling transcription cofactor Pygopus (Pygo) (Kramps et al., 2002; Parker et al., 2002; Thompson et al., 2002) or Tnks under identical conditions in the adult intestine. Consistent with the results from *Tnks* mutant clones induced at the same stage, the percentage of multi-cell *pygo* null mutant clones increased significantly compared with wild-type control clones and was even greater than that observed in *Tnks* mutants (Fig. 3C). These findings support the hypothesis that the increased number of ISCs in *Tnks* mutants resulted from inactivation of Wingless signaling within intestinal compartments.

To further test the hypothesis that Tnks promotes Wingless signaling in the adult intestine, we analyzed reporters for the Wingless pathway target genes *naked* (*nkd*) and *frizzled 3* (*fz3*) (Olson et al., 2011; Sato et al., 1999; Sivasankaran et al., 2000; Zeng et al., 2000). Previous studies revealed that the *nkd-lacZ* and the *fz3-RFP* reporters are expressed in overlapping regional gradients along the length of the adult intestine and indicated that Wingless pathway activity is highest at all the major boundaries that exist between compartments (Fig. 4A,B) (Buchon et al., 2013; Tian et al., 2016). Both reporters also revealed that Wingless pathway activity gradually diminishes to a low level with distance from the boundaries and is maintained at low levels throughout midgut compartments (Tian et al., 2016). Furthermore, both reporters are expressed in ECs, and this expression is completely lost upon

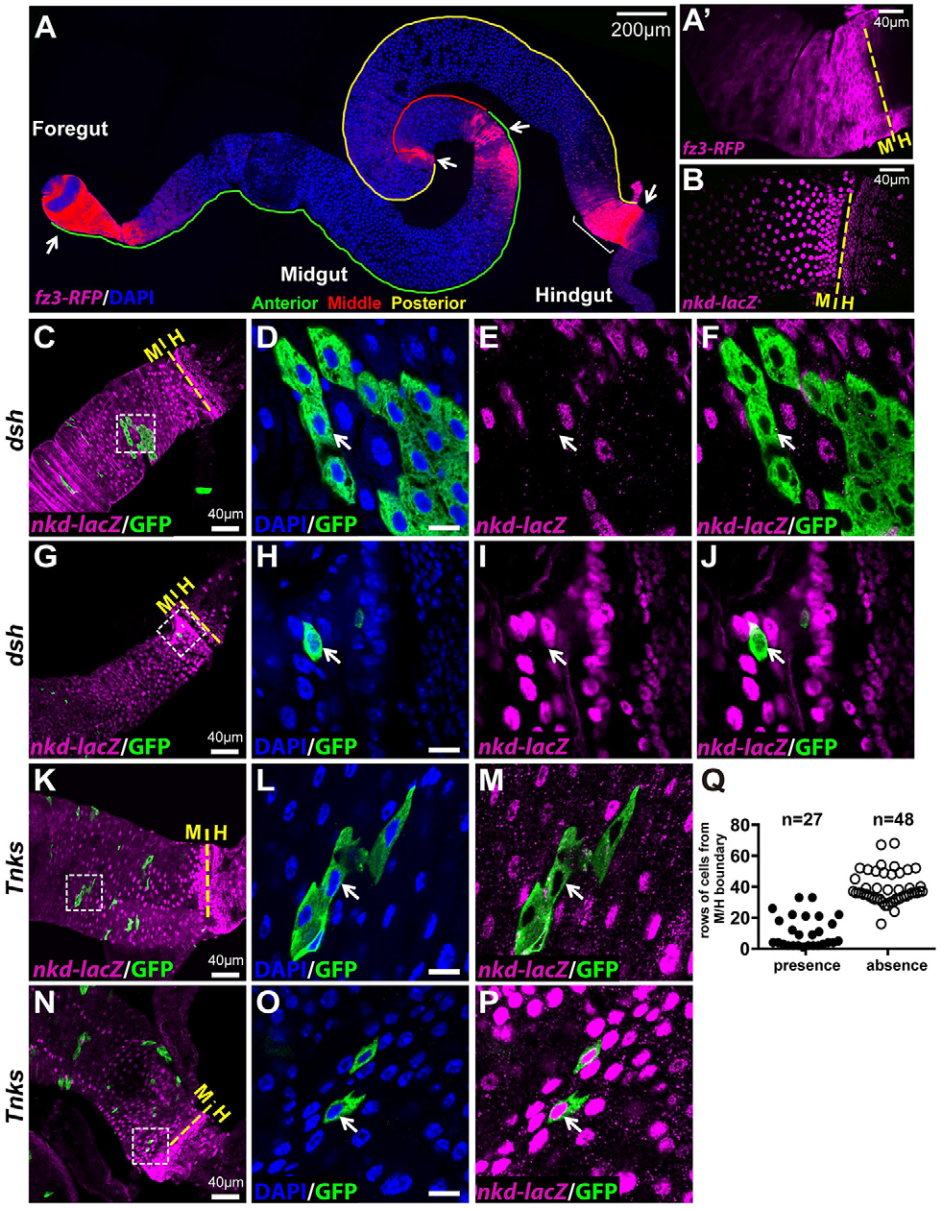

Fig. 4. Tnks promotes Wingless target gene activation in regions where the pathway activity is relatively low. (A) *fz3-RFP* is expressed in gradients at several compartment boundaries (arrow) in midguts. (A′) Higher magnification image of the *fz3-RFP* gradient (magenta) near the midgut/hindgut (M/H) boundary (bracket in A) reveals that *fz3-RFP* is expressed in progenitor cells and ECs. (B) *nkd-lacZ* (magenta) also forms a gradient near the midgut/hindgut boundary, but is expressed only in ECs. (C-J) *nkd-lacZ* expression is dependent on Wingless signaling activation. Null mutant clones of *dishevelled* (*dsh*), an essential Wingless pathway component, are marked by GFP. *nkd-lacZ* (magenta) is absent in *dsh* mutant ECs (arrow) both away from the compartment boundary (C-F) and near the boundary (G-J). (K-P) Tnks is required for *nkd-lacZ* expression in regions away from the compartment boundary (K-M), but is dispensable near the boundary where Wingless pathway activity is high (N-P). Low magnification images are shown in C, G, K and N with yellow dashed line indicating the midgut/hindgut boundary. Higher magnification views of the boxed areas are shown on the right. Scale bars: 10 μm if not indicated. (Q) Analysis of *nkd-lacZ* expression in *Tnks* clones relative to the distance from the midgut/hindgut boundary. Number of clones examined is indicated.

Development (2016) 143, 1710-1720 doi:10.1242/dev.127647

inactivation of Wingless signaling (Tian et al., 2016) (Fig. 4C-J and Fig. S2E-L). *Fz3-RFP* is also expressed in ISCs but this expression is independent of Wingless signaling in nearly all ISCs during homeostasis (Tian et al., 2016) (Fig. S2A-D). Thus, this previous work revealed that ECs are the primary cell type in which the Wingless pathway is activated under basal conditions during homeostasis.

To determine whether Tnks promotes Wingless signaling in the adult midgut, we tested whether the activation of Wingless target gene expression is dependent on Tnks. Using clonal analysis, we found that within compartments, where Wingless signaling activity is relatively low, *nkd-lacZ* expression was lost in *Tnks* mutant ECs (Fig. 4K-M). However, at the compartment boundaries, where Wingless pathway activity is high, the expression of *nkd-lacZ* was lost in *dsh* mutant cells (Fig. 4G-J), but retained in *Tnks* mutant cells (Fig. 4N-P). Spatial analysis of *Tnks* mutant clones revealed that Tnks was required for *nkd-lacZ* expression in ECs that were away from the midgut/hindgut boundary, but was dispensable for *nkd-lacZ* expression in ECs near the boundary, where Wingless pathway activity is high (Fig. 4Q). Similar results were obtained with the *fz3-RFP* reporter (Fig. S2E-T). These results indicated that within the intestinal epithelium, Tnks is essential for signaling in regions with relatively low pathway activation, but not required for Wingless target gene activation in regions with high levels of Wingless pathway activation.

Regulation of Axin by Tnks controls ISC proliferation

Together, these findings demonstrate that similar defects in regulation of ISC proliferation arise from inactivation of either Tnks or Wingless pathway components and provide the first evidence using null alleles that Tnks is important for the activation of Wingless target genes in a physiological context. We next tested whether this role of Tnks in promoting Wingless signaling reflects its negative regulation of Axin levels *in vivo*. However, the existing Axin antibodies did not allow detection of endogenous Axin in immunoblots, which was a presumed consequence of the very low Axin concentration (Tolwinski et al., 2003; Willert et al., 1999). We therefore generated a new antibody, which enabled sensitive detection of endogenous Axin; its specificity was demonstrated by the loss of Axin signal in lysates from *Axin* (*Axn*) null mutant larvae rescued to viability by a higher molecular weight Flag-Axin fusion protein (Fig. 5A). Using this antibody, we detected increased levels of Axin in lysates from *Tnks* mutant midguts compared with the wild type (Fig. 5B), consistent with the hypothesis that Tnks promotes Axin degradation *in vivo*.

Therefore, we sought to determine whether the overproliferation of ISCs in *Tnks* mutants resulted from increased Axin levels. We reasoned that if this were true, reduction of the *Axn* gene dosage might suppress the increased number of progenitor cells present in *Tnks* mutants. Indeed, the number of progenitor cells was restored to almost wild-type levels in *Tnks* mutants upon reduction of the *Axn* dosage by one-half (Fig. 5C-F). Consistently, reduction of the *Axn* gene dosage suppressed the proliferation of ISCs, as indicated by the reduced number of pH3^{+} cells (Fig. 5G). We also tested whether reducing the *Axn* gene dosage by half would suppress the aberrantly increased size of *Tnks* mutant clones. Because the *Tnks* and *Axn* genes are located on the same chromosomal arm, we performed this analysis by introduction of one copy of a *BAC-Axin-V5* transgene, in which Axin is expressed from its endogenous promoter (Gerlach et al., 2014), in *Tnks* and *Axn* double-null mutant clones. We found that the size of *Tnks* mutant clones was decreased significantly when the *Axn* gene dosage was reduced (Fig. 5H). These findings further support the hypothesis that increased Axin levels resulting from loss of Tnks inhibit Wingless signaling *in vivo* and thereby result in ISC overproliferation.

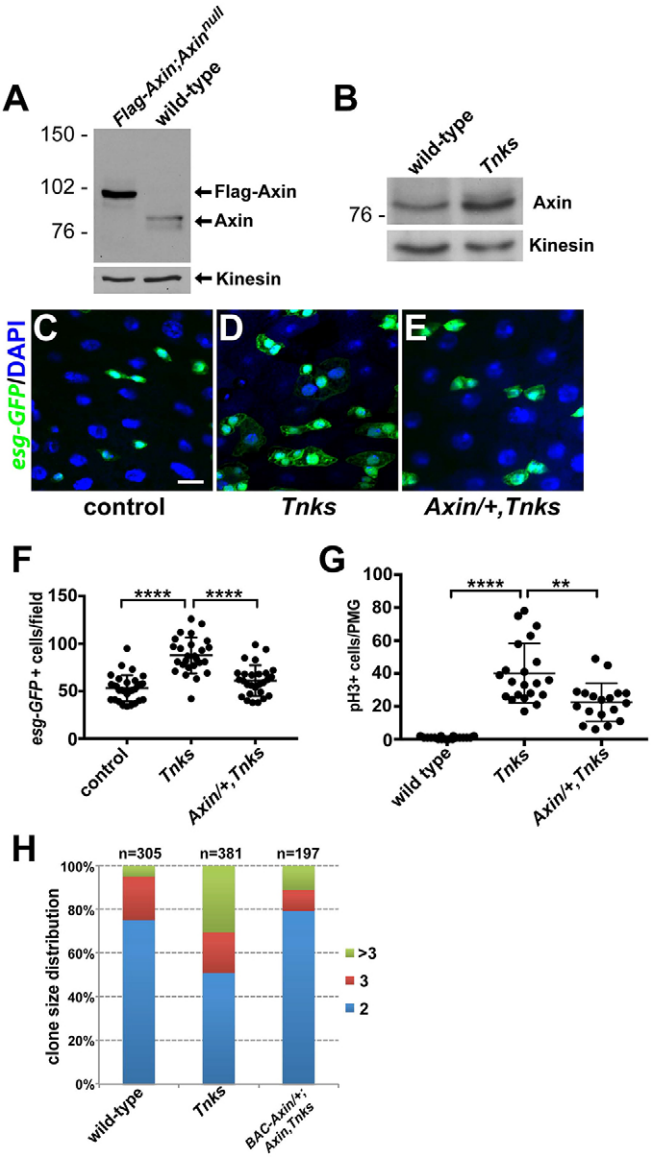

Fig. 5. Regulation of Axin by Tnks is required for control of ISC proliferation. (A) Detection of endogenous Axin by immunoblotting. Endogenous Axin is detected only in the wild-type larvae. *Axn*^{s044230} null mutant flies rescued to viability by expression of a *tub>Flag-Axn* transgene were used as a negative control for antibody specificity. Only the slower-migrating Flag-tagged Axin is present in these lysates, which are devoid of endogenous Axin. Kinesin was used as a loading control. (B) Axin protein levels are increased in *Tnks* mutants. Midgut lysates prepared from 5-day-old adult females of indicated genotypes immunoblotted with Axin antibody. (C-E) Reducing the *Axn* gene dosage by half restores the number of *esg>GFP*$^{+}$ progenitor cells. 5-day-old female flies of indicated genotypes expressing *esg>GFP* stained with anti-GFP (green) antibody and DAPI. Scale bar: 10 µm. (F) Quantification of the relative number of *esg>GFP*$^{+}$ ISCs and EBs cells from adult flies of indicated genotypes. *Tnks*$^{503/+}$ flies were used as control. (G) Quantification of pH3^{+} cells in posterior midguts from adult flies of indicated genotypes. Each dot represents an animal and lines indicate mean±s.d. ****P<0.0001 and **P<0.01 (t-test). (H) Reducing the *Axn* dosage by one-half restores the number of multi-cell *Tnks* mutant clones. Quantification of clone size for ISC lineages of indicated genotypes. Clones were induced in adults on the day of eclosion and analyzed 4 days later. Number of clones examined is indicated.

Development (2016) 143, 1710-1720 doi:10.1242/dev.127647

Regulation of Wingless signaling by Tnks in ECs non-autonomously controls proliferation of neighboring ISCs

Our previous work revealed that under basal homeostatic conditions, the Wingless pathway is activated primarily in ECs and that inactivation of Wingless signaling in ECs resulted in the overproliferation of neighboring ISCs in a non-autonomous manner (Tian et al., 2016). Therefore, we sought to determine whether the loss of Tnks, like that of other Wingless pathway components, non-autonomously promotes the proliferation of neighboring ISCs. We induced either wild-type control clones or *Tnks* mutant clones during adulthood and identified progenitor cells with the *esg-lacZ* reporter. In wild-type clones, progenitor cells were distributed evenly along the midgut (Fig. 6A-C). However, in *Tnks* mutant clones induced at the same stage, an aberrantly increased number of wild-type progenitor cells was present in proximity to the mutant clones (Fig. 6D-F,J). Similar results were obtained when *pygo* mutant clones were induced in adulthood (Fig. 6G-J) (Tian et al., 2016), supporting the hypothesis that loss of Tnks results in the inactivation of Wingless signaling. By contrast, no defects were observed when *Tnks* mutant clones were induced during pupation and analyzed at eclosion (Fig. S3). Together, these findings raised the possibility that the increase in ISCs caused by loss of Tnks resulted from inactivation of Wingless signaling in neighboring ECs.

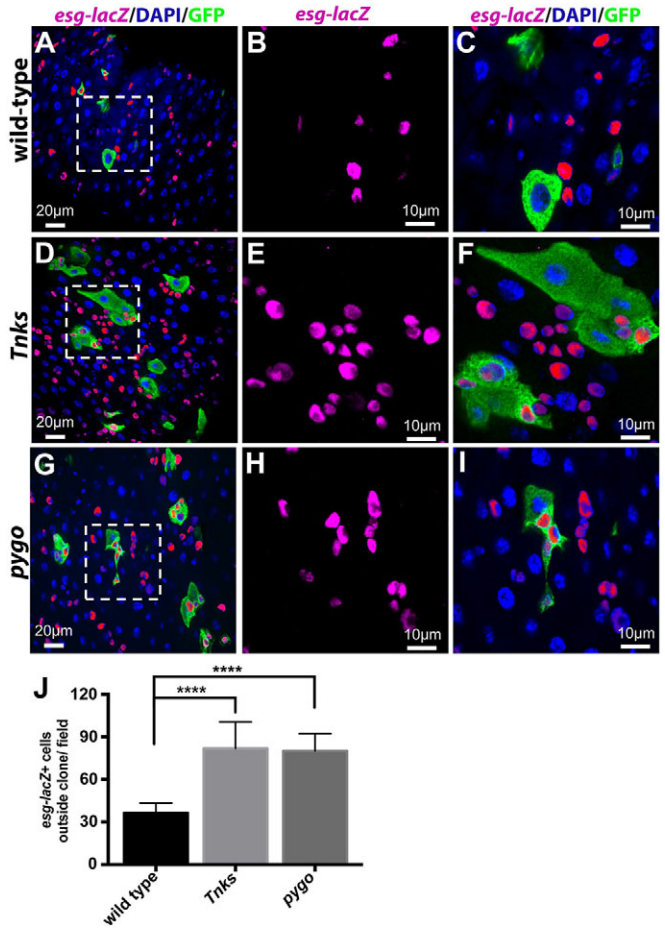

Fig. 6. Loss of Tnks non-autonomously promotes the proliferation of neighboring ISCs. Progenitor cells (marked by *esg-lacZ*) in adult midguts with MARCM clones of indicated genotypes. Clones were induced in adults on the day of eclosion and examined 4 days later. Wild-type clones have no effects on the neighboring ISCs (A-C), whereas $Tnks^{503}$ (D-F) or $pygo^{S123}$ (G-I) null mutant clones result in the overproliferation of neighboring ISCs, as revealed by the increased number of $esg\text{-}lacZ^{+}$ cells. (B,C,E,F,H,I) Higher magnification views of the boxed areas in the left panels. (J) Quantification of the relative number of progenitor cells outside the clones of indicated genotypes. n=11, 15, 17 for each genotype respectively. ****P<0.0001 (t-test). Error bars indicate s.d.

To directly test this hypothesis, we disrupted Tnks function specifically in either ECs or progenitor cells using RNAi-mediated *Tnks* knockdown. We used *Myo1A-Gal4* or *esg-Gal4* and the temperature-sensitive Gal4 repressor $Gal80^{ts}$ (McGuire et al., 2004) (together referred to as $Myo1A^{ts}$-*Gal4* or esg^{ts}-*Gal4*) to induce the temporal knockdown of *Tnks* in either ECs or progenitor cells, respectively (Jiang et al., 2009; Micchelli and Perrimon, 2006). On the day of eclosion, flies were shifted to the restrictive temperature (29°C) for 7 days and midguts were analyzed subsequently. As reported previously (Ohlstein and Spradling, 2006), ISCs and EBs were identified by their smaller size, high level of membrane-associated Armadillo/β-catenin, and lack of nuclear Prospero staining (which was used to distinguish pre-EE and EE cells from ISCs) (Fig. S4). Compared with controls (Fig. 7A,D), knockdown of *Tnks* in ECs resulted in an increased number of progenitor cells, which is consistent with overproliferation of ISCs (Fig. 7A-B′,D). Indeed, the number of $pH3^{+}$ cells increased significantly in these animals compared with controls, further supporting the conclusion that inactivation of Tnks in ECs results in the non-autonomous overproliferation of ISCs (Fig. 7E). By contrast, no defects were observed when *Tnks* was knocked down in progenitor cells (Fig. 7C,D). The same findings were observed with a second, independently derived *Tnks* RNAi line (Feng et al., 2014), ruling out the possibility of RNAi off-target effects (Fig. 7D,E and Fig. S5A-B′). As reported previously, disruption of Wingless signaling specifically in ECs, through RNAi-mediated knockdown of essential components of the Wingless pathway, similarly leads to an increased number of ISCs, whereas their knockdown in progenitor cells has no observed effect (Fig. S5C-D′) (Tian et al., 2016).

To further test the importance of Tnks function in ECs for the non-autonomous regulation of ISC proliferation, we expressed a *Tnks-HA* transgene in ECs using the *Myo1A-Gal4* driver. Quantification of Delta $(Dl)^{+}$ ISCs revealed that expressing *Tnks-HA* in ECs is sufficient to suppress the increased number of ISCs in *Tnks* mutants (Fig. 7F). As expected, the increase in $pH3^{+}$ cells was also suppressed by the expression of *Tnks-HA* in ECs (Fig. 7G). Together, these results further supported the conclusion that Tnks loss inactivates Wingless signaling in ECs, and thereby results in the non-autonomous induction of ISC overproliferation.

Non-autonomous control of JAK/STAT signaling in ISCs by Wingless pathway activation in ECs requires Tnks

To test the possibility that loss of Tnks results in midgut apoptosis, thus causing compensatory overproliferation of ISCs, we stained *Tnks* mutant midguts with an antibody against the cleaved Dcp-1 caspase. The specificity of the Dcp-1 antibody was confirmed by staining the midguts of control flies expressing *rpr* (*reaper*) in ECs (Fig. S6A-D′). However, no ectopic expression of Dcp-1 was observed in *Tnks* mutants (Fig. S6E-F′), ruling out the presence of aberrant apoptosis.

Thus, we hypothesized that inactivation of Tnks in ECs resulted in the aberrant activation of unknown signal transduction pathway(s) in neighboring ISCs, and thereby induced their overproliferation. Previous studies had revealed that several signal transduction pathways are important to control ISC proliferation, in particular the JAK/STAT, epidermal growth factor (EGF) and Decapentaplegic (Dpp)/TGF-β pathways (Biteau and Jasper, 2011; Guo et al., 2013; Jiang et al., 2011, 2009; Li et al., 2013b; Tian and Jiang, 2014; Xu

Development (2016) 143, 1710-1720 doi:10.1242/dev.127647

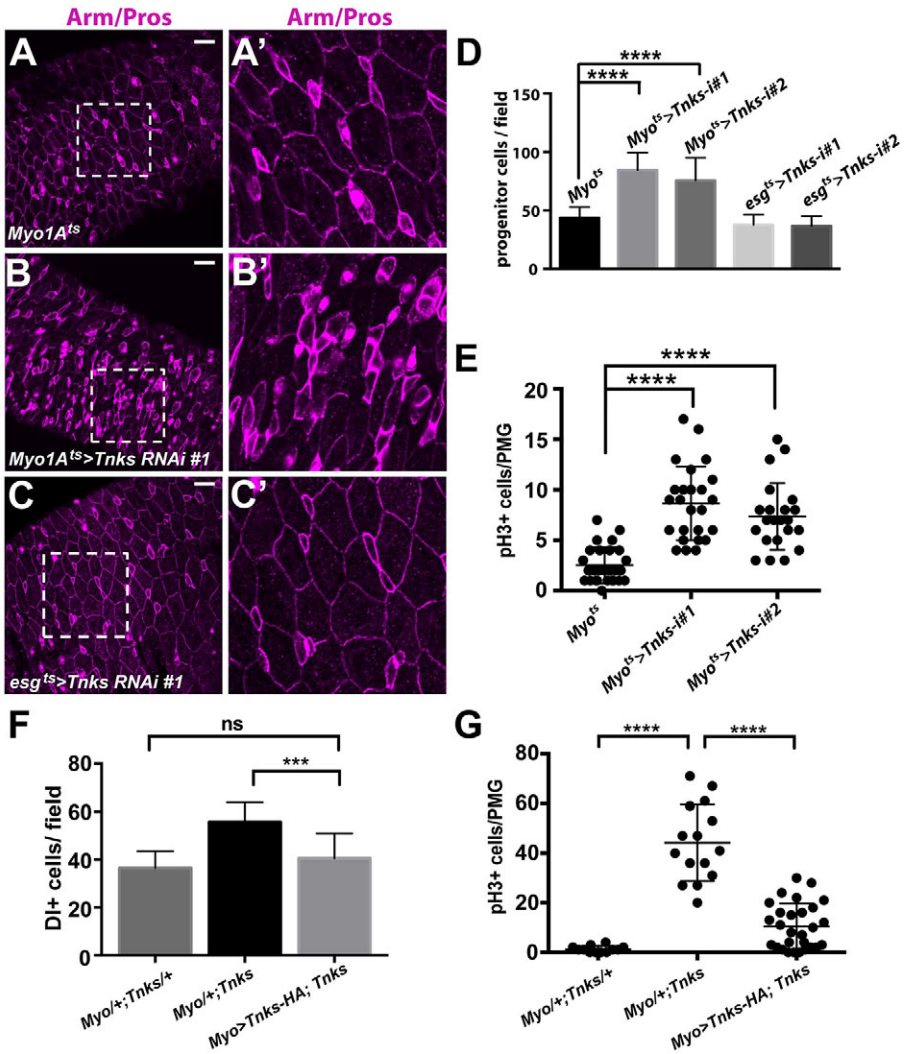

Fig. 7. Tnks is important in ECs to prevent ISC overproliferation. Adults expressing *Tnks-RNAi* #1 (B,B′) in ECs have increased number of progenitor cells compared with controls (A,A′), whereas those expressing the siRNAs in progenitor cells (C,C′) have no defects. (A′-C′) Higher magnification views of the boxed areas in A-C, respectively. Scale bars: 20 µm. (D) Quantification of the relative number of progenitor cells for flies of indicated genotype. *n*=13, 12, 13, 19 and 18 for each genotype, respectively. Error bars indicate s.d. *****P*<0.0001 (*t*-test). (E) Quantification of pH3$^+$ cells in posterior midguts from flies of indicated genotypes. Each dot represents an animal and lines indicate means±s.d. *****P*<0.0001 (*t*-test). (F) Expression of *Tnks-HA* transgene in ECs suppress the increased number of ISCs in *Tnks* mutants. Quantification of the relative number of ISCs for flies of indicated genotype. *n*=14, 18 and 18 for each genotype, respectively. Error bars indicate s.d. ****P*<0.001; ns, not significant (*t*-test). (G) Quantification of pH3$^+$ cells in posterior midguts from 14-day-old flies of indicated genotypes. Each dot represents an animal and lines indicate means ±s.d. *****P*<0.0001 (*t*-test).

et al., 2011). We therefore examined whether knockdown of *Tnks* in ECs resulted in increased expression of the ligands from these pathways using RT-qPCR. Indeed, we observed a 5- to 6-fold, and 3- to 4-fold increase in the levels of *unpaired 2* and *3* (*upd2* and *upd3*), respectively, two ligands of the JAK/STAT pathway that are expressed in ECs, whereas *keren* (*krn*) and *dpp* expression (ligands for EGF and TGF-β pathway, respectively) were increased only 1.5- to 2-fold (Fig. 8A). Similarly, previous work had revealed that RNAi-mediated knockdown of the Wingless pathway components Arrow, Pygo or Tcf (Parker et al., 2002; Thompson et al., 2002; van de Wetering et al., 1997; Wehrli et al., 2000) in ECs also resulted in a preferential increase in *upd2* and *upd3* expression (Tian et al., 2016). Together, these findings suggested that loss of Tnks in ECs disrupts Wingless signaling and thereby results in the aberrant activation of JAK/STAT signaling in ISCs.

To test this hypothesis directly, we analyzed a *stat-GFP* reporter to monitor the activation of JAK/STAT signaling (Bach et al., 2007). In wild-type posterior midguts, *stat-GFP* is expressed primarily in ISCs. However, in guts bearing *Tnks* mutant clones, the level of *stat-GFP* expression in ISCs was markedly increased both within and near the clones (Fig. 8B-E), indicating that the JAK/STAT pathway had been aberrantly activated in a non-autonomous manner. Similarly, we recently reported that the level of *stat-GFP* expression was aberrantly increased in ISCs by inactivation of Wingless signaling and this effect was found both within and near the clones (Tian et al., 2016) (Fig. S7). To determine whether the ectopic expression of Upd in ECs is responsible for the overproliferation of ISCs in *Tnks* mutants, we knocked down *upd3* in ECs using two different RNAi lines and found that knockdown of *upd3* was sufficient to suppress the increased number of ISCs in *Tnks* mutants (Fig. 8F). Consistently, knockdown of *upd3* in *Tnks* mutants restored the proliferation rate of ISCs to wild-type levels, as indicated by the number of pH3$^+$ cells (Fig. 8G). Taken together, these findings demonstrated that the disruption of Wingless signaling resulting from loss of Tnks in ECs induces the non-autonomous activation of JAK/STAT signaling in neighboring ISCs, and thereby results in their aberrant proliferation (Fig. 8H).

DISCUSSION

Despite the recent focus on Tnks inhibitors as potential therapeutic agents for Wnt-driven cancers, the *in vivo* contexts in which Tnks is required to promote Wnt signaling have remained uncertain. Here, we addressed the function of the sole *Drosophila* Tnks protein in the regulation of ISC proliferation. This approach capitalized on fly genetics and circumvented the complications of functional redundancy in vertebrates. Our studies are the first to demonstrate, through analysis of null alleles under physiological conditions, that Tnks is essential for the same subset of Wingless-dependent

Development (2016) 143, 1710-1720 doi:10.1242/dev.127647

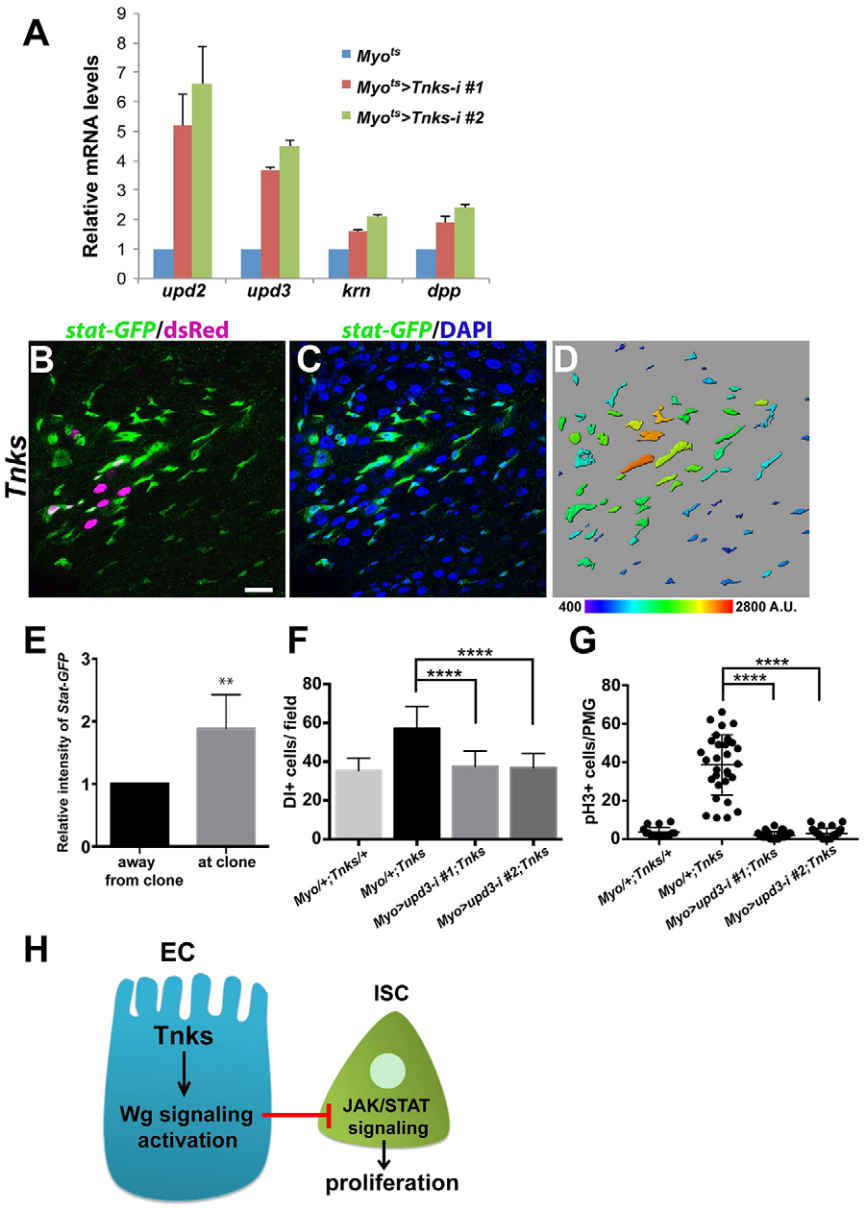

Fig. 8. Loss of Tnks non-autonomously activates JAK/STAT signaling to promote ISC proliferation. (A) Expression of *Tnks-RNAi* in ECs increased mRNA levels of the JAK/STAT pathway ligands *upd2* and *upd3*. Relative mRNA levels of *upd2*, *upd3*, *krn* and *dpp* in posterior midguts of the indicated genotypes measured by RT-qPCR. Value indicates fold activation relative to controls. *Myo1A*/+ flies were used as control. Error bars indicate s.d. (B-D) Expression of *stat-GFP* in midguts with $Tnks^{503}$ clones (marked by dsRed). *stat-GFP* (green) is ectopically expressed in progenitor cells adjacent to $Tnks^{503}$ clones (magenta), compared with regions further away from the clones. (D) Color-coded representation of *stat-GFP* intensity. Scale bar: 20 µm. (E) Quantification of relative intensity of *stat-GFP* in regions away from the clones and in regions at the clones. n=5 and error bars indicate s.d. $^{**}P$<0.01 (t-test). (F) Knockdown of *upd3* in ECs suppresses the increased number of ISCs in *Tnks* mutants. Quantification of the relative number of ISCs for flies of indicated genotype. n=18, 25, 26 and 29 for each genotype, respectively. Error bars indicate s.d. $^{****}P$<0.0001 (t-test). (G) Quantification of $pH3^{+}$ cells in posterior midguts from 14-day-old flies of indicated genotypes. Each dot represents an animal and lines indicate means±s.d. $^{****}P$<0.0001 (t-test). (H) A working model for the regulation of ISC proliferation by Tnks. Tnks is important for the activation of Wingless signaling in ECs. The activation of Wingless signaling inhibits activation of JAK/STAT pathway in neighboring ISCs non-autonomously, which controls their proliferation.

processes that control ISC proliferation (Tian et al., 2016). Furthermore, our results reveal that the requirement for Tnks is spatially restricted to regions of relatively low Wingless pathway activation *in vivo*. Finally, we show that, like Wingless pathway components (Tian et al., 2016), Tnks prevents the non-autonomous activation of the JAK/STAT pathway in ISCs, and thereby prevents their aberrant proliferation. Together, our findings suggest that Tnks is essential for the Wingless-dependent control of ISC proliferation and thus for the maintenance of intestinal homeostasis, and elucidate the underlying mechanism.

This work builds on the recent discovery that the activation of the Wingless pathway is graded along the length of the adult intestine, peaking at distinct compartment boundaries, but also present at low levels throughout intestinal compartments (Buchon et al., 2013; Tian et al., 2016). We find that Tnks is not required unconditionally for signaling throughout the entire length of these gradients of Wingless pathway activity. Indeed, Tnks is essential for Wingless target gene activation and the control of ISC proliferation within compartments, where the levels of Wingless pathway activation are relatively low, but is dispensable for target gene activation at compartment boundaries, where Wingless pathway activity peaks. On the basis of these findings, we postulate that the spatially restricted requirement for Tnks reflects its role in the amplification of signaling. At low levels of Wingless pathway activation, the nuclear level of β-catenin might be near the threshold required for target gene activation and the increased Axin levels resulting from Tnks inactivation would lower β-catenin levels below this critical threshold. By contrast, at high Wingless concentration, β-catenin levels would surpass the threshold necessary for target gene activation, even following loss of Tnks. This spatially restricted requirement for Tnks might explain disparities in recent *in vivo* studies regarding the requirement for Tnks in Wnt-directed physiological processes (Feng et al., 2014; Huang et al., 2009). Furthermore, our studies might have relevance for Tnks function in Wnt gradients in vertebrates, such as in the graded activation of the Wnt pathway along mammalian intestinal crypts. Moreover, the efficacy of Tnks inhibitors could reflect an essential function for Tnks in the amplification of pathway activity in Wnt-driven cancers.

Development (2016) 143, 1710-1720 doi:10.1242/dev.127647

Depletion of Tnks has no obvious effects on wing development or the expression of Wingless target genes in larval wing discs unless Axin levels are raised above the endogenous level (Feng et al., 2014; Wang et al., 2016). The threshold at which Axin levels inhibit Wingless signaling in wing discs is between 3- and 9-fold above the endogenous Axin level (Wang et al., 2016) and more than 3-fold in embryos (Yang et al., 2016). However, the phenotypes resulting from loss of Tnks in the midgut resemble those resulting from disruption of the Wingless pathway and are rescued by reducing the *Axn* gene dosage. This finding suggests Tnks is crucial to maintain Axin levels below a physiological threshold and thus to ensure proper activation of Wingless signaling in midgut, and suggest that the threshold at which Axin levels disrupt signaling is lower in the adult intestine compared with other tissues. Alternatively, other mechanisms may promote Axin degradation to compensate for Tnks loss in other tissues or developmental stages, whereas such compensatory mechanisms might not exist in the adult intestine. As intestinal homeostasis is disrupted in *Tnks* mutants, the physiological functions of the midgut, primarily in digestion and absorption of nutrients, are likely to be impaired. Under standard lab conditions, *Tnks* mutant flies exhibit no obvious survival disadvantage when compared with wild-type flies. However, with limited nutrient supply, the integrity of the midgut becomes vital for maintaining organismal fitness.

Previous studies indicated that Wingless pathway activation is required autonomously for long-term ISC self-renewal and for ISC proliferation upon tissue damage (Cordero et al., 2012; Lin et al., 2008). In addition, Wingless pathway activation in ECs controls ISC proliferation non-autonomously, and is thereby crucial to maintain intestinal homeostasis (Tian et al., 2016). Here, we have found that like Wingless pathway components, Tnks is essential for this process; Tnks inactivation disrupts the expression of Wingless target genes in ECs, leading to the hyperactivation of the JAK/STAT pathway and thereby the overproliferation of nearby ISCs. As observed for other Wingless pathway components, inactivation of *Tnks* in mutant clones results in aberrantly increased proliferation of neighboring ISCs. In addition, like other Wingless components, knockdown of *Tnks* specifically in ECs, but not in progenitors, results in ISC overproliferation, further supporting this non-autonomous mechanism. These findings suggest that to ensure proper proliferation of ISCs during homeostasis, the Wingless pathway status in ECs must be tightly regulated in a process that requires Tnks.

As the intestine serves as a crucial barrier against pathogens and toxins, the maintenance of intestinal integrity is essential for survival. Many conserved signal transduction pathways regulate ISC behavior following injury, including the EGF, JAK/STAT, Wingless/Wnt, TGF-β/Dpp and insulin pathways (Biteau and Jasper, 2011; Choi et al., 2011; Cordero et al., 2012; Guo et al., 2013; Jiang et al., 2011, 2009; Lee et al., 2009; Li et al., 2013b; O'Brien et al., 2011; Tian and Jiang, 2014; Xu et al., 2011). The interplay between these different signaling pathways ensures homeostatic renewal as well as rapid regenerative responses to injury. We provide evidence that loss of Tnks in ECs upregulates expression of *upd2* and *upd3* and thereby induces the aberrant activation of JAK/STAT signaling in ISCs, placing Wingless signaling upstream of the JAK/STAT pathway in the non-autonomous regulation of ISC proliferation. Therefore, this Tnks-dependent mechanism ensures that JAK/STAT signaling is largely repressed in ISCs under basal conditions, but is poised for rapid activation during the regenerative response to intestinal injury.

MATERIALS AND METHODS

Flies and genetics

The $Tnks^{503}$ and $Tnks^{19}$ mutants were isolated as described in supplementary Materials and Methods. Other stocks used were: *esg-Gal4, UAS-GFP* (Micchelli and Perrimon, 2006), esg^{K606} (Micchelli and Perrimon, 2006), *Su(H)GBE-lacZ* (Micchelli and Perrimon, 2006), *fz3-RFP* (Olson et al., 2011), *nkd-lacZ* (Zeng et al., 2000), *10× stat-GFP* (Bach et al., 2007), *hs-flp, UAS-mCD8:GFP; tub-Gal4, FRT82B, tub-Gal80* (Li et al., 2013a), *hs-flp, tub-gal4, UAS-dsRed; FRT82B, tub-gal80* (Guo et al., 2013), *hs-flp, tub-Gal80, FRT19A; tub-Gal4, UAS-mCD8:GFP* (Choi et al., 2011), *FRT82B* (BDSC), *82B* $pygo^{S123}$ (Thompson et al., 2002), dsh^{V26} *FRT19A* (Klingensmith et al., 1994; Wehrli and Tomlinson, 1998), *tub>Flag-Axin;* $Axin^{s044230}$ (Peterson-Nedry et al., 2008), $Axin^{s044230}$ (Hamada et al., 1999), *BAC Axin-V5* integrated at the VK30 site (PBac{y[+]-attP-9A}VK00030) (Gerlach et al., 2014), *Myo1A-Gal4* (Karpowicz et al., 2013), *Myo1A-Gal4, tub-Gal80*^{ts}*, UAS-GFP* (Jiang et al., 2009), *esg-Gal4, tub-Gal80*^{ts}*, UAS-GFP* (Micchelli and Perrimon, 2006), *UAS-Tnks RNAi#1* (VDRC#106238), *UAS-Tnks RNAi#2* (*Tnks-RNAi-2*) (Feng et al., 2014), *UAS-dsh RNAi* (VDRC#31306), *UAS-upd3 RNAi#1* (VDRC#106869), *UAS-upd3 RNAi#2* (VDRC#27136), *UAS-rpr3-5/TM3*. Canton S flies were used as controls, and all crosses were performed at 25°C unless otherwise indicated. Only adult female flies were analyzed in this study.

Clonal analysis and RNAi experiments

Mitotic clones were generated using the MARCM system (Lee and Luo, 2001). Adult flies were subjected to a 30 min heat shock in a 37°C water bath on the day of eclosion. *dsh* mutant clones were induced by two 2 h heat shocks, with at least 3 h between consecutive heat shocks. After heat shock, flies were maintained at 25°C for 4-6 days before analysis. For analysis of *fz3-RFP* expression (Fig. 4 and Fig. S2), clones were induced in 3rd instar larvae by a single 2 h heat shock and examined 1-2 days after eclosion, as *fz3-RFP* expression becomes less homogenous with age. For quantification of clone size, only clones in the posterior midgut were included in the analysis (Fig. 3C and Fig. 5G). For RNAi experiments, crosses were maintained at 22°C and progeny of desired genotypes were collected on the day of eclosion and kept at 29°C for 7 or 10 days before dissection.

Antibodies

Antibodies against Axin and Tnks were generated as described in supplementary Materials and Methods. Both antibodies were used at 1:1000 for immunoblots. Other primary antibodies used were chicken anti-GFP (Abcam, ab13970, 1:10,000), mouse anti-Arm (DSHB, 1:20), mouse anti-Prospero (DSHB, 1:100), mouse anti-Delta (DSHB, 1:100), rabbit anti-dsRed (Clontech, 632496, 1:1000), mouse anti-β-gal (Promega, Z3788, 1:5000), rabbit anti-β-gal (MP Biomedicals, 559762, 1:5000), rabbit anti-Pdm1 (Lee et al., 2009) (gift from Dr Xiaohang Yang, Institute of Molecular and Cell Biology, Singapore, 1:200), rabbit anti-phospho-histone H3 (Ser10) (Millipore, 06-570, 1:1000), rabbit anti-cleaved Dcp-1 (Cell Signaling, 9578S 1:100), rabbit anti-Kinesin Heavy Chain (Cytoskeleton, AKIN01-A, 1:10,000 for immunoblots). Secondary antibodies used for immunostaining were goat or donkey Alexa Fluor 488 or 555 conjugates (Invitrogen, 1:400) and goat Cy5 conjugates (Jackson ImmunoResearch, 1:200). Secondary antibodies used for immunoblots were goat anti-guinea pig HRP-conjugates (Jackson ImmunoResearch, 1:5000) or goat anti-rabbit HRP-conjugates (Bio-Rad, 1:10,000).

Immunostaining and immunoblots

For immunostaining, adult intestines were dissected in PBS, fixed in 4% paraformaldehyde in PBS for 45 min. For Delta staining, intestines were fixed in 8% formaldehyde, 200 mM sodium cacodylate, 100 mM sucrose, 40 mM potassium acetate, 10 mM sodium acetate and 10 mM EGTA for 20 min at room temperature (O'Brien et al., 2011). Tissues were then washed in PBS with 0.1% Triton X-100, followed by incubation in PBS with 0.1% Tween-20 and 10% BSA for 1 h at room temperature. Incubation with primary antibodies was performed at 4°C overnight in PBS with 0.5% Triton X-100. Incubation with secondary antibodies was for 2 h at room temperature. Specimens were mounted in Prolong Gold (Invitrogen).

Development (2016) 143, 1710-1720 doi:10.1242/dev.127647

Fluorescent images were obtained on a Nikon A1RSi confocal microscope and processed using Adobe Photoshop software.

For midgut lysates used in immunoblots, midguts from 5-day-old adults were dissected in cold PBS, and then treated with 1× Trypsin in EDTA (Corning Life Sciences) for 2 h at room temperature. Tissues were washed with PBS and homogenized in 4× Laemmli loading buffer. Lysates were incubated for 5 min at 100°C before SDS-PAGE analysis.

RT-qPCR

Adult females were shifted to 29°C after eclosion for 7 days before analysis. Total RNA was extracted from 35 posterior midguts and cDNA was synthesized using M-MLV reverse transcriptase (Invitrogen). cDNA was analyzed in triplicate using the StepOnePlus Real-Time PCR system (Applied Biosystems). Expression of the target genes was measured relative to that of *rpl32* (*rp49*). Experiments were performed three times with independent biological samples and representative results are shown in Fig. 8A. Primers used are listed in supplementary Materials and Methods.

Life-span assay

For the life-span assay, 5-day-old wild-type or $Tnks^{19/503}$ mutant flies were placed in empty vials containing a 4×2.5 cm piece of chromatography paper. As a feeding medium, 400 µl of 5% sucrose solution was applied to the paper. Flies were transferred to new vials with fresh sucrose solution each day. Sixty flies of each genotype were used in this assay and 15 flies were placed in each vial. Experiments were performed at 29°C.

Quantification and statistics

For ISC quantification, flies were stained with anti-Delta and anti-Prospero antibodies. Images of the R5a region (Buchon et al., 2013) were obtained with a 60× objective and the total number of Dl^+ cells in a field of 0.023 mm^2 were counted. Progenitor cells were identified by *esg>GFP* (Fig. 5F), *esg-lacZ* (Fig. 6J) or by their smaller size, strong membrane-associated Arm and absence of nuclear Prospero (Fig. 7D). For quantification, the total number of progenitor cells (Fig. 5F and Fig. 7D), or progenitor cells outside indicated clones (Fig. 6J), was counted in a field of 0.032 mm^2 within R5a. In *Tnks* mutants, in which some ECs were also marked by *esg>GFP*, only progenitor cells were counted. For quantification of $pH3^+$ cells, the total number of $pH3^+$ cells in the posterior midgut of the indicated genotypes was counted. For quantification of *stat-GFP* immunostaining intensity, each *stat-GFP*$^+$ cell was identified using Imaris software (Bitplane). The mean intensity in cells within a field (40 µm×40 µm) surrounding a *Tnks* mutant clone or an equal field at least 50 µm away from the clone was measured. The relative intensity was calculated and shown in Fig. 8E. All *t*-tests were performed using Prism (GraphPad).

Acknowledgements

We thank Benjamin Ohlstein, Julia Cordero, Craig Micchelli, Ramanuj DasGupta, Norbert Perrimon, Claude Desplan, Konrad Basler, Matthew Scott, Yanrui Jiang, Jean-Paul Vincent, Xinhua Lin, Gary Struhl, Bruno Lemaitre, Xiaohang Yang and Yu Cai for kind gifts of flies and reagents. We also thank the Bloomington Stock Center and the Vienna Drosophila Research Center for fly stocks, the Drosophila Genomics Resource Center and Developmental Studies Hybridroma Bank for reagents. We thank Lucy Erin O'Brien, Rongwen Xi, Julia Cordero and Bruno Lemaitre for providing protocols and advice, Victoria Marlar, Arvonn Tully, and Ann Lavanway for technical support, and Girish Deshpande and Claudio Pikielny for thoughtful comments on the manuscript.

Competing interests

The authors declare no competing or financial interests.

Author contributions

Z.W., A.T., H.B. and Y.A. conceived the study. Z.W., A.T., H.B., O.T.-B., E.Y. and Y.A. designed and performed the experiments. H.N. provided reagents. Z.W. and Y.A. wrote the manuscript.

Funding

This work was funded by grants from the Office of Extramural Research, National Institutes of Health [RO1CA105038 to Y.A., P40OD018537 to the BDSC], the Emerald Foundation (to Y.A.), the Norris Cotton Cancer Center (to Y.A.) and the National Science Foundation [DBI-1039423 for the purchase of a Nikon A1RSi confocal microscope]. Deposited in PMC for release after 12 months.

Supplementary information

Supplementary information available online at
http://dev.biologists.org/lookup/suppl/doi:10.1242/dev.127647/-/DC1

References

Bach, E. A., Ekas, L. A., Ayala-Camargo, A., Flaherty, M. S., Lee, H., Perrimon, N. and Baeg, G.-H. (2007). GFP reporters detect the activation of the Drosophila JAK/STAT pathway in vivo. *Gene Expr. Patterns* **7**, 323-331.

Beehler-Evans, R. and Micchelli, C. A. (2015). Generation of enteroendocrine cell diversity in midgut stem cell lineages. *Development* **142**, 654-664.

Biteau, B. and Jasper, H. (2011). EGF signaling regulates the proliferation of intestinal stem cells in Drosophila. *Development* **138**, 1045-1055.

Biteau, B. and Jasper, H. (2014). Slit/Robo signaling regulates cell fate decisions in the intestinal stem cell lineage of Drosophila. *Cell Rep.* **7**, 1867-1875.

Buchon, N., Osman, D., David, F. P. A., Yu Fang, H., Boquete, J.-P., Deplancke, B. and Lemaitre, B. (2013). Morphological and molecular characterization of adult midgut compartmentalization in Drosophila. *Cell Rep.* **3**, 1725-1738.

Chen, B., Dodge, M. E., Tang, W., Lu, J., Ma, Z., Fan, C.-W., Wei, S., Hao, W., Kilgore, J., Williams, N. S. et al. (2009). Small molecule–mediated disruption of Wnt-dependent signaling in tissue regeneration and cancer. *Nat. Chem. Biol.* **5**, 100-107.

Chiang, Y. J., Hsiao, S. J., Yver, D., Cushman, S. W., Tessarollo, L., Smith, S. and Hodes, R. J. (2008). Tankyrase 1 and tankyrase 2 are essential but redundant for mouse embryonic development. *PLoS ONE* **3**, e2639.

Choi, N. H., Lucchetta, E. and Ohlstein, B. (2011). Nonautonomous regulation of Drosophila midgut stem cell proliferation by the insulin-signaling pathway. *Proc. Natl. Acad. Sci. USA* **108**, 18702-18707.

Clevers, H. and Nusse, R. (2012). Wnt/beta-catenin signaling and disease. *Cell* **149**, 1192-1205.

Cordero, J. B., Stefanatos, R. K., Scopelliti, A., Vidal, M. and Sansom, O. J. (2012). Inducible progenitor-derived Wingless regulates adult midgut regeneration in Drosophila. *EMBO J.* **31**, 3901-3917.

Feng, Y., Li, X., Ray, L., Song, H., Qu, J., Lin, S. and Lin, X. (2014). The Drosophila tankyrase regulates Wg signaling depending on the concentration of Daxin. *Cell. Signal.* **26**, 1717-1724.

Fevr, T., Robine, S., Louvard, D. and Huelsken, J. (2007). Wnt/beta-catenin is essential for intestinal homeostasis and maintenance of intestinal stem cells. *Mol. Cell. Biol.* **27**, 7551-7559.

Gerlach, J. P., Emmink, B. L., Nojima, H., Kranenburg, O. and Maurice, M. M. (2014). Wnt signalling induces accumulation of phosphorylated beta-catenin in two distinct cytosolic complexes. *Open Biol.* **4**, 140120.

Guo, Z., Driver, I. and Ohlstein, B. (2013). Injury-induced BMP signaling negatively regulates Drosophila midgut homeostasis. *J. Cell Biol.* **201**, 945-961.

Hamada, F., Tomoyasu, Y., Takatsu, Y., Nakamura, M., Nagai, S.-i., Suzuki, A., Fujita, F., Shibuya, H., Toyoshima, K., Ueno, N. et al. (1999). Negative regulation of Wingless signaling by D-axin, a Drosophila homolog of axin. *Science* **283**, 1739-1742.

Huang, S.-M. A., Mishina, Y. M., Liu, S., Cheung, A., Stegmeier, F., Michaud, G. A., Charlat, O., Wiellette, E., Zhang, Y., Wiessner, S. et al. (2009). Tankyrase inhibition stabilizes axin and antagonizes Wnt signalling. *Nature* **461**, 614-620.

Ireland, H., Kemp, R., Houghton, C., Howard, L., Clarke, A. R., Sansom, O. J. and Winton, D. J. (2004). Inducible Cre-mediated control of gene expression in the murine gastrointestinal tract: effect of loss of beta-catenin. *Gastroenterology* **126**, 1236-1246.

Jiang, H. and Edgar, B. A. (2011). Intestinal stem cells in the adult Drosophila midgut. *Exp. Cell Res.* **317**, 2780-2788.

Jiang, H., Patel, P. H., Kohlmaier, A., Grenley, M. O., McEwen, D. G. and Edgar, B. A. (2009). Cytokine/Jak/Stat signaling mediates regeneration and homeostasis in the Drosophila midgut. *Cell* **137**, 1343-1355.

Jiang, H., Grenley, M. O., Bravo, M.-J., Blumhagen, R. Z. and Edgar, B. A. (2011). EGFR/Ras/MAPK signaling mediates adult midgut epithelial homeostasis and regeneration in Drosophila. *Cell Stem Cell* **8**, 84-95.

Karpowicz, P., Zhang, Y., Hogenesch, J. B., Emery, P. and Perrimon, N. (2013). The circadian clock gates the intestinal stem cell regenerative state. *Cell Rep.* **3**, 996-1004.

Klingensmith, J., Nusse, R. and Perrimon, N. (1994). The Drosophila segment polarity gene dishevelled encodes a novel protein required for response to the wingless signal. *Genes Dev.* **8**, 118-130.

Korinek, V., Barker, N., Morin, P. J., van Wichen, D., de Weger, R., Kinzler, K. W., Vogelstein, B. and Clevers, H. (1997). Constitutive transcriptional activation by a beta -catenin-Tcf complex in APC-/- colon carcinoma. *Science* **275**, 1784-1787.

Korinek, V., Barker, N., Moerer, P., van Donselaar, E., Huls, G., Peters, P. J. and Clevers, H. (1998). Depletion of epithelial stem-cell compartments in the small intestine of mice lacking Tcf-4. *Nat. Genet.* **19**, 379-383.

Kramps, T., Peter, O., Brunner, E., Nellen, D., Froesch, B., Chatterjee, S., Murone, M., Züllig, S. and Basler, K. (2002). Wnt/wingless signaling requires

BCL9/legless-mediated recruitment of pygopus to the nuclear beta-catenin-TCF complex. *Cell* **109**, 47-60.
Lau, T., Chan, E., Callow, M., Waaler, J., Boggs, J., Blake, R. A., Magnuson, S., Sambrone, A., Schutten, M., Firestein, R. et al. (2013). A novel tankyrase small-molecule inhibitor suppresses APC mutation-driven colorectal tumor growth. *Cancer Res.* **73**, 3132-3144.
Lee, T. and Luo, L. (2001). Mosaic analysis with a repressible cell marker (MARCM) for Drosophila neural development. *Trends Neurosci.* **24**, 251-254.
Lee, W.-C., Beebe, K., Sudmeier, L. and Micchelli, C. A. (2009). Adenomatous polyposis coli regulates Drosophila intestinal stem cell proliferation. *Development* **136**, 2255-2264.
Li, X., Erclik, T., Bertet, C., Chen, Z., Voutev, R., Venkatesh, S., Morante, J., Celik, A. and Desplan, C. (2013a). Temporal patterning of Drosophila medulla neuroblasts controls neural fates. *Nature* **498**, 456-462.
Li, Z., Zhang, Y., Han, L., Shi, L. and Lin, X. (2013b). Trachea-derived dpp controls adult midgut homeostasis in Drosophila. *Dev. Cell* **24**, 133-143.
Lin, G., Xu, N. and Xi, R. (2008). Paracrine Wingless signalling controls self-renewal of Drosophila intestinal stem cells. *Nature* **455**, 1119-1123.
Lum, L. and Clevers, H. (2012). Cell biology. The unusual case of Porcupine. *Science* **337**, 922-923.
MacDonald, B. T., Tamai, K. and He, X. (2009). Wnt/beta-catenin signaling: components, mechanisms, and diseases. *Dev. Cell* **17**, 9-26.
McGuire, S. E., Mao, Z. and Davis, R. L. (2004). Spatiotemporal gene expression targeting with the TARGET and gene-switch systems in Drosophila. *Sci. STKE* **2004**, pl6.
Micchelli, C. A. and Perrimon, N. (2006). Evidence that stem cells reside in the adult Drosophila midgut epithelium. *Nature* **439**, 475-479.
Morin, P. J., Sparks, A. B., Korinek, V., Barker, N., Clevers, H., Vogelstein, B. and Kinzler, K. W. (1997). Activation of beta -catenin-Tcf signaling in colon cancer by mutations in beta -catenin or APC. *Science* **275**, 1787-1790.
Morrone, S., Cheng, Z., Moon, R. T., Cong, F. and Xu, W. (2012). Crystal structure of a Tankyrase-Axin complex and its implications for Axin turnover and Tankyrase substrate recruitment. *Proc. Natl. Acad. Sci. USA* **109**, 1500-1505.
O'Brien, L. E., Soliman, S. S., Li, X. and Bilder, D. (2011). Altered modes of stem cell division drive adaptive intestinal growth. *Cell* **147**, 603-614.
Ohlstein, B. and Spradling, A. (2006). The adult Drosophila posterior midgut is maintained by pluripotent stem cells. *Nature* **439**, 470-474.
Ohlstein, B. and Spradling, A. (2007). Multipotent Drosophila intestinal stem cells specify daughter cell fates by differential notch signaling. *Science* **315**, 988-992.
Olson, E. R., Pancratov, R., Chatterjee, S. S., Changkakoty, B., Pervaiz, Z. and DasGupta, R. (2011). Yan, an ETS-domain transcription factor, negatively modulates the Wingless pathway in the Drosophila eye. *EMBO Rep.* **12**, 1047-1054.
Pare, A. C., Dean, D. M. and Ewer, J. (2009). Construction and characterization of deletions with defined end points in Drosophila using P elements in trans. *Genetics* **181**, 53-63.
Parker, D. S., Jemison, J. and Cadigan, K. M. (2002). Pygopus, a nuclear PHD-finger protein required for Wingless signaling in Drosophila. *Development* **129**, 2565-2576.
Parks, A. L., Cook, K. R., Belvin, M., Dompe, N. A., Fawcett, R., Huppert, K., Tan, L. R., Winter, C. G., Bogart, K. P., Deal, J. E. et al. (2004). Systematic generation of high-resolution deletion coverage of the Drosophila melanogaster genome. *Nat. Genet.* **36**, 288-292.
Peterson-Nedry, W., Erdeniz, N., Kremer, S., Yu, J., Baig-Lewis, S. and Wehrli, M. (2008). Unexpectedly robust assembly of the Axin destruction complex regulates Wnt/Wg signaling in Drosophila as revealed by analysis in vivo. *Dev. Biol.* **320**, 226-241.
Qian, L., Mahaffey, J. P., Alcorn, H. L. and Anderson, K. V. (2011). Tissue-specific roles of Axin2 in the inhibition and activation of Wnt signaling in the mouse embryo. *Proc. Natl. Acad. Sci. USA* **108**, 8692-8697.
Sato, A., Kojima, T., Ui-Tei, K., Miyata, Y. and Saigo, K. (1999). Dfrizzled-3, a new Drosophila Wnt receptor, acting as an attenuator of Wingless signaling in wingless hypomorphic mutants. *Development* **126**, 4421-4430.
Sbodio, J. I., Lodish, H. F. and Chi, N.-W. (2002). Tankyrase-2 oligomerizes with tankyrase-1 and binds to both TRF1 (telomere-repeat-binding factor 1) and IRAP (insulin-responsive aminopeptidase). *Biochem. J.* **361**, 451-459.
Sivasankaran, R., Calleja, M., Morata, G. and Basler, K. (2000). The Wingless target gene Dfz3 encodes a new member of the Drosophila Frizzled family. *Mech. Dev.* **91**, 427-431.
Smith, S., Giriat, I., Schmitt, A. and de Lange, T. (1998). Tankyrase, a poly(ADP-ribose) polymerase at human telomeres. *Science* **282**, 1484-1487.
Thompson, B., Townsley, F., Rosin-Arbesfeld, R., Musisi, H. and Bienz, M. (2002). A new nuclear component of the Wnt signalling pathway. *Nat. Cell Biol.* **4**, 367-373.
Tian, A. and Jiang, J. (2014). Intestinal epithelium-derived BMP controls stem cell self-renewal in Drosophila adult midgut. *eLife* **3**, e01857.
Tian, A., Benchabane, H., Wang, Z. and Ahmed, Y. (2016). Regulation of stem cell proliferation and cell fate specification by wingless/Wnt signaling gradients enriched at adult intestinal compartment boundaries. *PLoS Genet.* **12**, e1005822.
Tolwinski, N. S., Wehrli, M., Rives, A., Erdeniz, N., DiNardo, S. and Wieschaus, E. (2003). Wg/Wnt signal can be transmitted through arrow/LRP5,6 and Axin independently of Zw3/Gsk3beta activity. *Dev. Cell* **4**, 407-418.
van de Wetering, M., Cavallo, R., Dooijes, D., van Beest, M., van Es, J., Loureiro, J., Ypma, A., Hursh, D., Jones, T., Bejsovec, A. et al. (1997). Armadillo coactivates transcription driven by the product of the Drosophila segment polarity gene dTCF. *Cell* **88**, 789-799.
van Es, J. H., Haegebarth, A., Kujala, P., Itzkovitz, S., Koo, B.-K., Boj, S. F., Korving, J., van den Born, M., van Oudenaarden, A., Robine, S. et al. (2012). A critical role for the Wnt effector Tcf4 in adult intestinal homeostatic self-renewal. *Mol. Cell. Biol.* **32**, 1918-1927.
Waaler, J., Machon, O., Tumova, L., Dinh, H., Korinek, V., Wilson, S. R., Paulsen, J. E., Pedersen, N. M., Eide, T. J., Machonova, O. et al. (2012). A novel tankyrase inhibitor decreases canonical Wnt signaling in colon carcinoma cells and reduces tumor growth in conditional APC mutant mice. *Cancer Res.* **72**, 2822-2832.
Wang, Z., Tacchelly-Benites, O., Yang, E., Thorne, C. A., Nojima, H., Lee, E. and Ahmed, Y. (2016). Wnt/Wingless pathway activation is promoted by a critical threshold of Axin maintained by the tumor suppressor APC and the ADP-ribose polymerase Tankyrase. *Genetics.* **203**, 1-13.
Wehner, D. and Weidinger, G. (2015). Signaling networks organizing regenerative growth of the zebrafish fin. *Trends Genet.* **31**, 336-343.
Wehrli, M. and Tomlinson, A. (1998). Independent regulation of anterior/posterior and equatorial/polar polarity in the Drosophila eye; evidence for the involvement of Wnt signaling in the equatorial/polar axis. *Development* **125**, 1421-1432.
Wehrli, M., Dougan, S. T., Caldwell, K., O'Keefe, L., Schwartz, S., Vaizel-Ohayon, D., Schejter, E., Tomlinson, A. and DiNardo, S. (2000). arrow encodes an LDL-receptor-related protein essential for Wingless signalling. *Nature* **407**, 527-530.
Willert, K., Shibamoto, S. and Nusse, R. (1999). Wnt-induced dephosphorylation of axin releases beta -catenin from the axin complex. *Genes Dev.* **13**, 1768-1773.
Xu, N., Wang, S. Q., Tan, D., Gao, Y., Lin, G. and Xi, R. (2011). EGFR, Wingless and JAK/STAT signaling cooperatively maintain Drosophila intestinal stem cells. *Dev. Biol.* **354**, 31-43.
Yang, E., Tacchelly-Benites, O., Wang, Z., Randall, M. P., Tian, A., Benchabane, H., Freemantle, S., Pikielny, C., Tolwinski, N. S., Lee, E. et al. (2016). Wnt pathway activation by ADP-ribosylation. *Nat. Commun.* **7**, 11430.
Zeng, X. and Hou, S. X. (2015). Enteroendocrine cells are generated from stem cells through a distinct progenitor in the adult Drosophila posterior midgut. *Development* **142**, 644-653.
Zeng, W., Wharton, K. A., Jr., Mack, J. A., Wang, K., Gadbaw, M., Suyama, K., Klein, P. S. and Scott, M. P. (2000). naked cuticle encodes an inducible antagonist of Wnt signalling. *Nature* **403**, 789-795.
Zielke, N., Korzelius, J., van Straaten, M., Bender, K., Schuhknecht, G. F. P., Dutta, D., Xiang, J. and Edgar, B. A. (2014). Fly-FUCCI: A versatile tool for studying cell proliferation in complex tissues. *Cell Rep.* **7**, 588-598.

Supplementary Materials and Methods

Flies and genetics

To isolate *Tnks* mutants, the transposase encoded by *P{Δ2-3}* (Robertson et al., 1988) (Bloomington Drosophila Stock Center (BDSC)) was used to mobilize the *P* element *G9172*, an EP insertion (Rorth, 1996) provided by KAIST, South Korea. We screened for deletions within the *Tnks* locus by PCR, which were confirmed by sequencing. $Tnks^{503}$ contains a deletion of 1859 nucleotides (-20 to +1839 with reference to the *Tnks* transcriptional start site). Approximately 3.3K nucleotides from *G9172* remain at this site. A deletion of the entire *Tnks* gene, $Tnks^{19}$, was isolated by hybrid element insertion (Pare et al., 2009; Parks et al., 2004), using *P{Δ2-3}HoP* (BDSC) to simultaneously mobilize the *P* elements *G9172* and *KG00687* (Bellen et al., 2004), which flank the *Tnks* gene. Prior to performing this screen, the recessive marker *scarlet (st)* was combined in *cis* with *KG00687*, and *claret (ca)* was combined in *cis* with *G9172* using meiotic recombination. To isolate potential deletions, we screened for *st ca* recombinants. $Tnks^{19}$ contains a deletion of 9089 nucleotides (-20 to +9069 with reference to the *Tnks* transcriptional start site).

Antibodies

To generate Axin polyclonal antibodies, a PCR fragment encoding amino acids 43 to 358 of the Axin protein was amplified by PCR from the *Axin* cDNA in *pAc5.1-Daxin-3xHA* (Huang et al., 2009), and ligated at the EcoRI site of *pPROEX HTb* vector (Invitrogen). To generate Tnks polyclonal antibody, a fragment encoding amino acids 423 to 885 (in the Ankyrin repeat region) of the Tnks protein was amplified by PCR from the *Tnks cDNA LD22548* (Drosophila Genomics Research Center), and inserted at the NcoI and NotI sites of the *pPROEX HTa* vector (Invitrogen). His-tag fusion proteins were purified

with TALON metal affinity resin (Clontech) and used as an immunogen in guinea pigs (Cocalico Biologicals). The Axin GP90 and Tnks GP96 antisera were used at a 1:1000 dilution for immunoblots.

RT-qPCR

The following primers were used to examine relative gene expression by RT-qPCR:

upd2: Forward primer: 5'-TGGTATTCGCTCATCGTGA-3'

Reverse primer: 5'-GGCAAATCA GAGATCCCG-3'

upd3: Forward primer: 5'-AGGCCATCAACCTGACCAAC-3'

Reverse primer: 5'-ACGCTTCTCCATCAGCTTGC-3'

krn: Forward primer: 5'-GTTGCTCCGCTAACAATGCT-3'

Reverse primer: 5'-GAACGATGGCACCTGCT-3'

dpp: Forward primer: 5'-TCTGCTGACCAAGTCGG-3'

Reverse primer: 5'-GCGGGAATGCTCTTCAC-3'

rpl32: Forward primer: 5'-AGGCCCAAGATCGTGAAGAA-3'

Reverse primer: 5'-TGTTGCACCAGGAACTTCTTGAA-3'

Supplementary References

Bellen, H.J., Levis, R.W., Liao, G., He, Y., Carlson, J.W., Tsang, G., Evans-Holm, M., Hiesinger, P.R., Schulze, K.L., Rubin, G.M., *et al*. (2004). The BDGP gene disruption project: single transposon insertions associated with 40% of Drosophila genes. Genetics *167*, 761-781.

Huang, S.M., Mishina, Y.M., Liu, S., Cheung, A., Stegmeier, F., Michaud, G.A., Charlat, O., Wiellette, E., Zhang, Y., Wiessner, S., *et al*. (2009). Tankyrase inhibition stabilizes axin and antagonizes Wnt signalling. Nature *461*, 614-620.

Pare, A.C., Dean, D.M., and Ewer, J. (2009). Construction and characterization of deletions with defined end points in Drosophila using P elements in trans. Genetics *181*, 53-63.

Parks, A.L., Cook, K.R., Belvin, M., Dompe, N.A., Fawcett, R., Huppert, K., Tan, L.R., Winter, C.G., Bogart, K.P., Deal, J.E., *et al*. (2004). Systematic generation of high-resolution deletion coverage of the Drosophila melanogaster genome. Nature genetics *36*, 288-292.

Robertson, H.M., Preston, C.R., Phillis, R.W., Johnson-Schlitz, D.M., Benz, W.K., and Engels, W.R. (1988). A stable genomic source of P element transposase in Drosophila melanogaster. Genetics *118*, 461-470.

Rorth, P. (1996). A modular misexpression screen in Drosophila detecting tissue-specific phenotypes. Proceedings of the National Academy of Sciences of the United States of America *93*, 12418-12422.

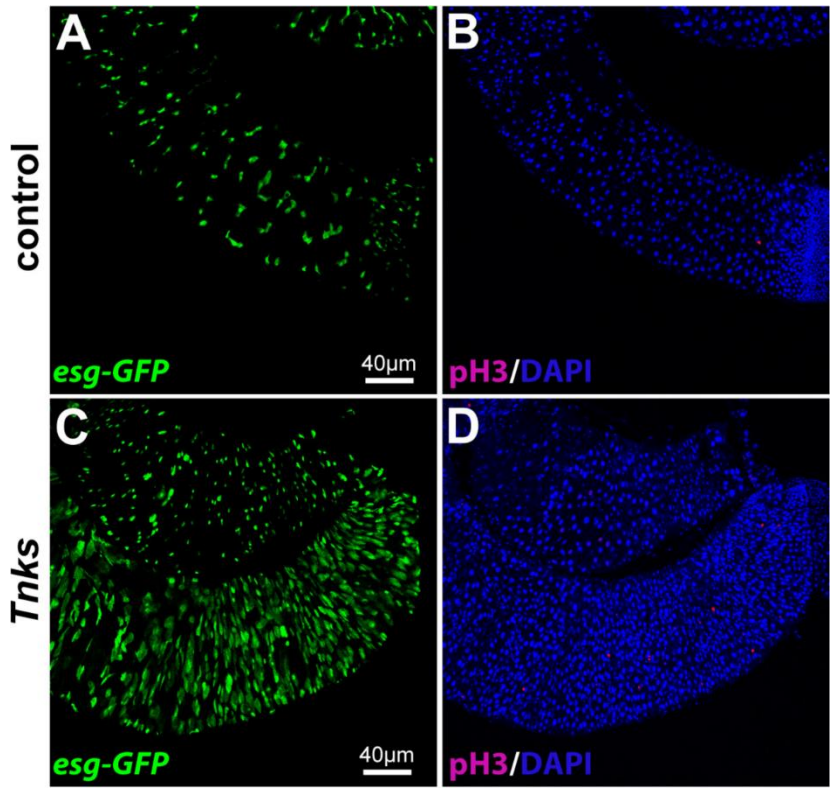

Fig S1: ISC overproliferation resulting from loss of Tnks increases in severity with age

Midguts of 14-day-old female flies expressing *esg>GFP* were stained with anti-phospho-histone H3 (magenta) and anti-GFP (GFP) antibodies. $Tnks^{19/503}$ mutants (C and D) have increased numbers of *esg-GFP*$^{+}$ and pH3^{+} cells compared with control flies ($Tnks^{503}$/+) (A and B).

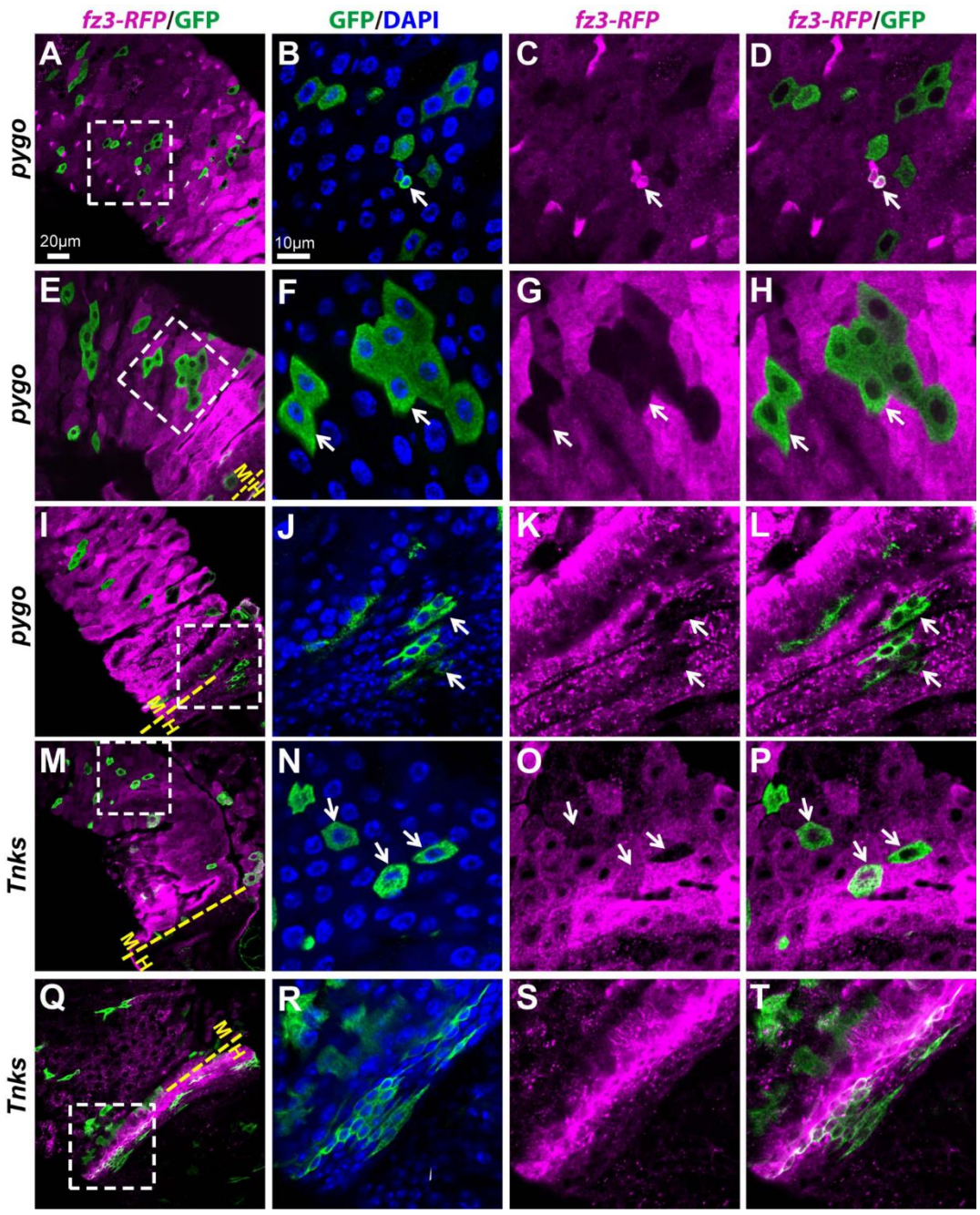

Fig S2: Tnks promotes Wingless target gene activation in regions where the pathway activity is relatively low

(A-D) *fz3-RFP* expression in ISCs is not dependent on Wingless signaling activation. $pygo^{S123}$ clones (marked by GFP) were induced in flies expressing *fz3-RFP*. *fz3-RFP* (magenta) remains the same in $pygo^{S123}$ mutant ISCs (arrow). (E-L) *fz3-RFp* expression in

ECs is dependent on Wingless signaling activation. *fz3-RFP* (magenta) is absent in *pygo*^{S123} mutant clones (arrows) both away from the compartment boundary (E-H) and near the boundary (I-L). (M-T) Tnks is required for *fz3-RFP* expression in regions away from the compartment boundary (M-P), but is dispensable near the boundary where Wingless pathway activity is high (Q-T). Mutant clones (marked by GFP) were induced in 3rd instar larvae and examined 1-2 days after eclosion. Low magnification images are shown in A, E, I, M and Q with yellow dashed line indicating the midgut/hindgut boundary. Higher magnification views of the boxed areas are shown on the right.

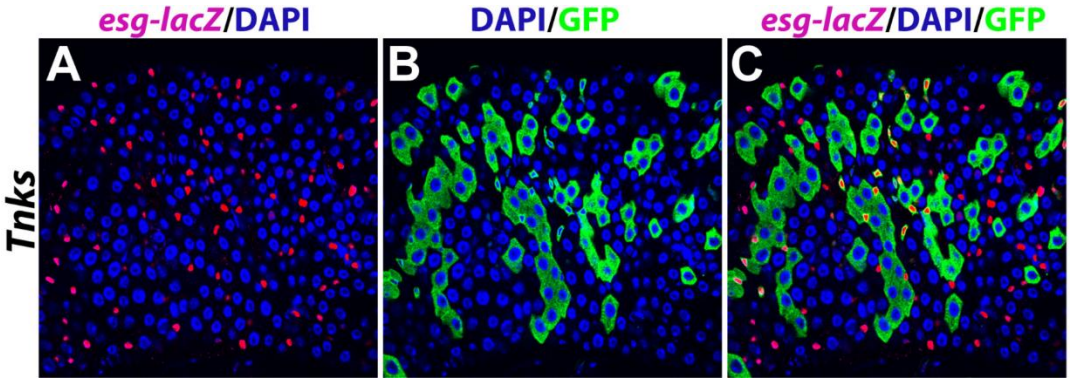

Fig S3: Loss of Tnks during pupal development has no effect on ISC proliferation at eclosion

Tnks clones (marked by GFP) were induced in 3rd instar larvae and analyzed on the day of eclosion. Progenitor cells, indicated by *esg-lacZ*, are evenly scattered along the midgut.

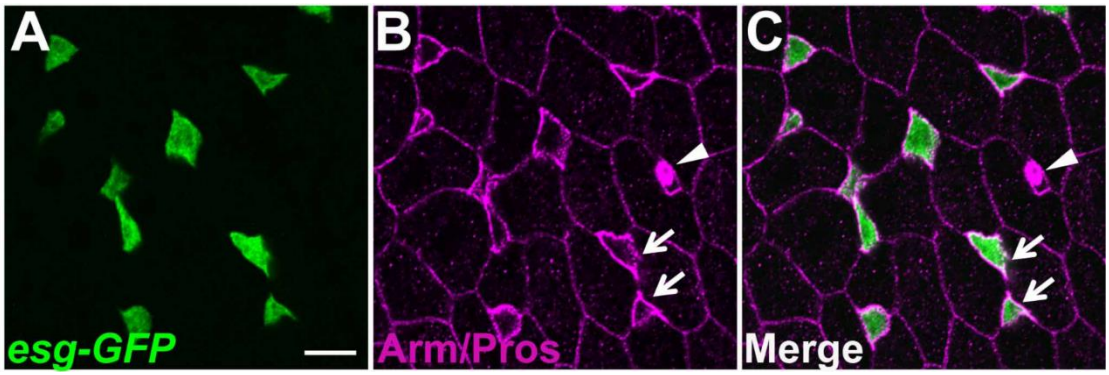

Fig S4: ISCs and EBs can be distinguished by their small size, high levels of membrane-associated Armadillo, and lack of nuclear Prospero

5-day-old female midguts expressing *esg-Gal4, UAS-GFP (esg>GFP)* were stained with anti-GFP (green), anti-Armadillo (Arm) (magenta) and anti-Prospero (magenta) antibodies. Progenitor cells (marked by *esg>GFP*) have smaller cell size and strong membrane-associated Arm staining (arrow). Differentiated EEs can be distinguished by Prospero staining (arrow head). Scale bar: 10μm.

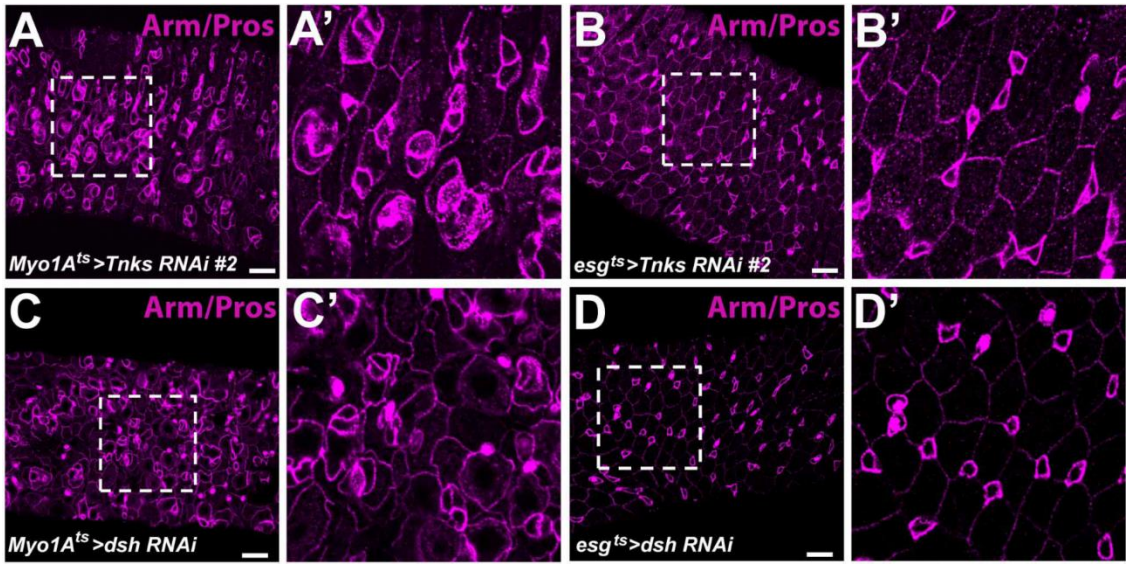

Fig S5: Loss of Tnks or Dishevelled (Dsh) in ECs causes overproliferation of ISCs

Knockdown of Tnks in ECs using the independent *Tnks-RNAi#2* line (A and A') results in overproliferation of ISCs; however, knockdown of Tnks in progenitor cells (B and B') using the same *Tnks-RNAi* line has no effects. Adults expressing *dsh RNAi* (C and C') in ECs display an increased number of progenitor cells, while those expressing the RNAis in progenitor cells (D and D') have no defects. Adult females were shifted to 29°C after eclosion for 7 days and midguts were stained with anti-Arm and anti-Prospero (magenta) antibodies. Scale bar: 20μm.

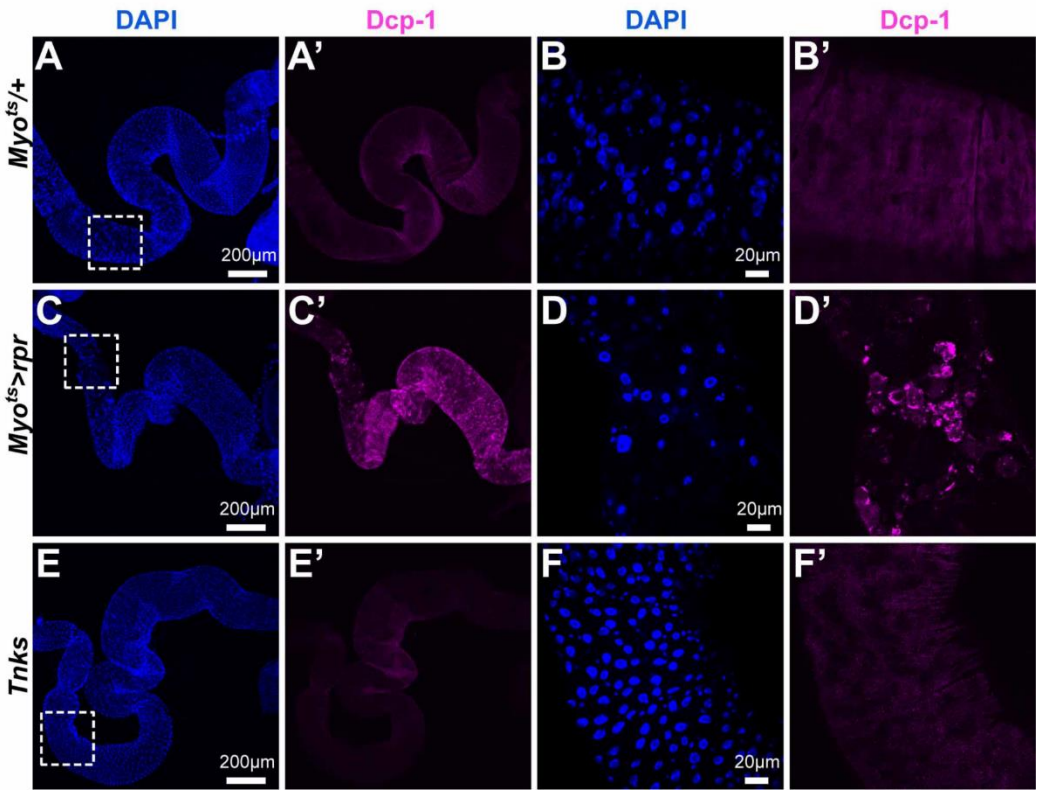

Fig S6: Loss of Tnks does not induce ectopic cell death

(A-D') Testing the specificity of Dcp-1 antibody. Three days after eclosion, control flies (*Myo^{ts}-Gal4*/+) or flies expressing *Myo^{ts}-Gal4, UAS-reaper* were shifted to 29°C for 42 hours and stained with Dcp-1 antibody. Ectopic Dcp-1 staining was observed when cell death was induced in ECs (C-D), but not in control flies (A-B). No ectopic expression of Dcp-1 was observed in *Tnks* mutant flies (E-F'). Low magnification images are shown in A, C and E. Higher magnification views of the boxed areas are shown in B, D and F. Images were obtained under the same setting.

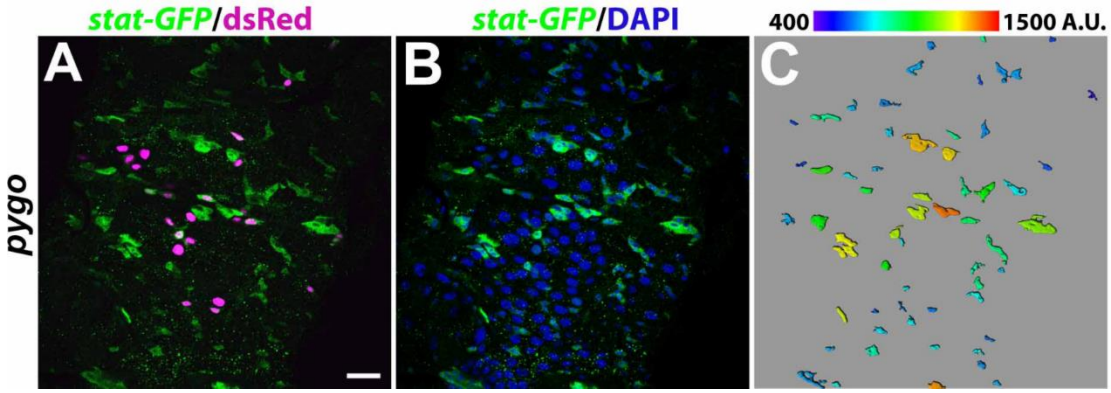

Fig S7: Loss of Pygo non-autonomously activates JAK/STAT signaling

(A-B) Expression of *stat-GFP* in midguts with $pygo^{S123}$ clones (magenta). *stat-GFP* (green) is expressed ectopically in progenitor cells adjacent to $pygo^{S12}$ clones (magenta), as compared to regions farther away from the clones. (C) Color-coded representation of *stat-GFP* intensity. Scale bar: 20µm.